TECHNICAL ANALYSIS OF EMPLOYING ON-SITE HYDROGEN PRODUCTION AND STORAGE SYSTEMS WITH RENEWABLE ENERGY FOR TELECOM SITES IN SRI LANKA

Laddu Wasana Dilrukshi

168509M

Degree of Master of Science

Department of Electrical Engineering

University of Moratuwa
Sri Lanka

March 2022

TECHNICAL ANALYSIS OF EMPLOYING ON-SITE HYDROGEN PRODUCTION AND STORAGE SYSTEMS WITH RENEWABLE ENERGY FOR TELECOM SITES IN SRI LANKA

Laddu Wasana Dilrukshi

168509M

Thesis submitted in partial fulfilment of the requirements for the degree Master of Science in Electrical Engineering

Department of Electrical Engineering

University of Moratuwa
Sri Lanka

March 2022

DECLARATION

I declare that it is indeed my own effort, and this thesis does not incorporate without affirmation any material previously submitted for a degree or Master's at any other college, university or institute of higher learning and to the best of my knowledge, that it does not comprise any material originally published or authored by another individual, except where acknowledgement is context specific.

In addition, I would like to grant the University of Moratuwa the non-exclusive right to procreate and publish my thesis, in whole or in section in print, electronic, or any other medium. I would like to retain the right to integrate this content into future works in whole or in part (such as articles or books).

…………………………… ….……………………

Signature of the candidate Date

(L.W. Dilrukshi)

The above candidate has carried out research for the Masters Thesis under my supervision.

…………………………… ……………………….

Signature of the supervisor Date

(Prof. K.T.M. Udayanga Hemapala)

ABSTRACT

Despite the fact that its technologies have grown at breakneck speed, energy is the lifeblood of the telecommunications industry. The concern is not only about how energy is delivered, but also about supply continuity and cost, all of which are key problems in the industry.

The telecommunications industry has begun to seek for renewable energy alternatives due to the rising cost of fossil fuels and the reliance on fossil fuels for commercial electricity. To overcome the inherent restrictions of renewable energy and maintain an uninterruptible power supply, the hydrogen storage idea was added into the renewable energy conversion system.

A fuel cell-based power system is explicitly modeled and studied in this study under different types of operating situations. The voltage output, current output, H_2 production, feed of air and fuel, pressure regulations, and flow rates must all be controlled in order to be technically feasible. The proposed methodology is valid for a PEMFC (Proton Exchange Membrane Fuel Cell) based power system, and the results are verified using the MATLAB Simulink tool.

Keywords: Technical analysis, fuel cell, Electrolyzer, H_2 storage, PEMFC, renewable energy, solar PV, Battery

ACKNOWLEDGEMENT

I would like to take the opportunity to share my sincere gratitude to all those who assisted me in successfully completing this research.

First and foremost, I would like to convey my sincere gratitude deeply to my supervisor Prof. K.T.M.U. Hemapala, Head, Department of Electrical Engineering, University of Moratuwa for the continuous support, proper guidance, constructive feedback, and encouragement from the commencement of this research until the completion of this thesis.

This work would not have been possible without the help of the post-graduate program's course coordinators and professors at the Department of Electrical Engineering, University of Moratuwa. Therefore, I appreciate the guidance and advice given by the evaluation panel.

Further, I would like to extend my gratitude to Mr. A.S. Anupama Silva for sharing vital data and information throughout the research period.

Also, my parents, brother, and friends deserve special thanks for their patience, understanding, and unwavering support.

TABLE OF CONTENTS

LIST OF FIGURES

LIST OF TABLES

LIST OF ABBREVIATIONS

PEMFC	Proton Exchange Membrane Fuel Cell
AFC	Alkaline Fuel cell
DMFC	Direct Methanol Fuel Cell
PAFC	Phosphoric Acid Fuel Cell
MCFC	Molten Carbonate Fuel Cell
SOFC	Solid Oxide Fuel Cell
PV	Photo Voltaic
SOC	State of Charge
CAN	Controller Area Network
UV	Ultraviolet
PRD	Pressure Relief Devices

CHAPTER 01

1. INTRODUCTION

1.1 Background Study

Since continuous supply of energy is the main vein of the telecommunication industry in an environment where the energy prices are constantly escalating, telecommunication operators are increasingly turning to renewable energy sources. The difficulty arises from the inherent constraints of typically renewable energy in the telecommunication business, which requires an uninterrupted supply of energy to the systems. When it comes to the intended use of renewable energy, solar and wind are the most widely accessible renewable energy sources, and this study focuses on solar as a renewable energy source.

When solar radiation is not available, at Sri Lankan base station sites, telecommunication providers frequently use a renewable energy system consists with a diesel generator and batteries to provide power. Solar energy is utilized to power the telecommunications equipment and the extra electricity is used to charge the batteries. When insolation is less or unable to reach, the devices are energized by the charged batteries. The diesel generator bridges the energy gap between demand and supply, with the surplus batteries are being charged for later use. These synchronizations are handled by devices called solar controllers.

Underneath these circumstances, the battery bank is subjected to cycles of intensive charging and discharging, resulting in a loss in battery lifespan. Furthermore, the diesel generator functions for the majority of the day.

In context of the aforesaid, it could be desirable to investigate methods to assist changes in the technique of harvesting solar energy and converting it into power for telecommunication base station sites in terms of sheer technological viability [3].

1.2 Statement of the Problem and justification

The battery banks' lifetime is greatly reduced as a result of the extensive charging-discharging cycles they undergo. As a result, a battery bank utilized with a standard sun-powered control system shall be typically replaced every 2-3 years, which has a significant cost impact on the location's operational consumption when the money-related execution is considered. In addition, the capital expenditure required for the diesel generator, as well as the scheduled maintenance required, are also impressive. Since the telecommunication industry in Sri Lanka is reasonably priced, the anticipated approach is having a substance to such broadcast communications industry's engineers and budgetary directors. It is worthwhile to undertake research to determine the available options for overcoming the aforementioned constraints while maintaining their specialized talents and financial viability in a viable circumstance [3].

1.3 Motivation to the Research

The goal of this project is to apply the Hydrogen capacity idea for a solar power system at a telecommunication base station location, as well as to investigate the operation of framework components. It will assist telecommunications decision-makers in selecting ideal framework components while minimizing the overall taken a toll of energy used for the operation by omitting batteries and optimizing the investment made in solar power framework deployment on base station sites.

1.4 Objectives of the Research

This research is intending to investigate the technical feasibility of substituting battery banks with hydrogen system for Telecom sites in Sri Lanka.

1.5 Methodology of the Research

The following segment is the synopsis of procedure followed to achieve objectives.

i. Survey on past literature

The previous research on Hydrogen generation combining with on-site insolation which uses renewable power for telecom base stations was reviewed.

ii. Data collection from the telecommunications network

To get a proper approach to the investigation, urgency of real data on actual practices captured with sun-power systems used in communication network sites in a Sri Lanka, is a necessity. In addition, determining the specialized applicability of the notion requires a common dispersal of control across base station sites in a communications network.

iii. Data collection on the concept's technological evolution in the industry

The modifications which are in-relate with proposed system components are to be examined of the compatibility with system, accessibility, and availability on market. This information is necessary for determining the concept's technical feasibility.

iv. System Modeling.

The system is modeled in MATLAB Simulink with the parameters of subjective data from base station sites to determine the best equipment sizes for the situation.

v. Defining cases for the simulation.

The study is characterizing states those were chosen based on the energy consumption of base station sites, as well as the dispersion of those locations vs the availability of four zones to transport an acceptable number of solar panels. When describing the states, the topographical conveyance of base station sites was taken into account to account for the practicality in the face of diverse insolation patterns.

vi. Results validation

The findings of MATLAB Simulink were authenticated with the specifications of the equipment, and outputs of hydrogen system and battery system were compared.

1.6 Outline of the Thesis

The outline of the document is as follow.

Chapter 2 introduces the background knowledge
Chapter 3 presents the gathered and analyzed data
Chapter 4 concludes the model of the system
Chapter 5 concludes the simulation results and analysis
Chapter 6 concludes the equipment selection
Chapter 7 concludes the safety related issues and best practices
Finally, Chapter 8 concludes the conclusion in this thesis and assumptions & limitations

CHAPTER 02

2 LITERATURE REVIEW

2.1 Hydrogen

The hydrogen particle is the lightest, least complex, and most normal component in the universe. In any case, it happens just in blend with different components, basically with oxygen in water and with carbon, nitrogen, and oxygen in living materials and petroleum products. Hydrogen is certainly not an essential wellspring of energy. Notwithstanding, it turns into an appealing energy transporter when parted from these different components by utilizing a wellspring of energy. Hydrogen, as perfect energy transporter, is viewed as the spotless fuel of future especially for energy stockpiling and transport. The energy stockpiling limit of hydrogen is amazing in light of the fact that computations show that one kilogram of hydrogen contains roughly 33 kWh of energy.

The upsides of hydrogen are: (i) energy security by diminishing oil imports, (ii) supportability by exploiting the RE sources, (iii) less contamination and better metropolitan air quality by delivering close to zero carbon, hydrocarbon, GHG and NOx outflows at the place of utilization, and (iv) monetary suitability by possibly forming the future worldwide energy markets. Along these lines, Hydrogen is an around the world acknowledged clean energy transporter as it is source-autonomous and has a high energy content for every mass contrasted with oil as recorded in Table below. Despite the fact that there are some nitrogen oxides created during high temperature burning, ecological toxin can be completely taken out during low temperature usage, for example, by power modules. Hydroelectricity-Hydrogen Energy System (HHES) can be utilized for energy to remote or disconnected regions like rustic towns, lodgings, wilderness locales and islands [12].

Table 2.1-1 Comparison between Hydrogen and different fuel as source of energy [12]

Fuel	Energy content (MJ/kg)	Fuel	Energy content (MJ/kg)
Hydrogen	120.0	Ethanol	29.6
Liquefied natural gas	54.4	Methanol	19.7
Propane	49.6	Coke	27.0
Automotive gasoline	46.4	Wood (dry)	16.2
Automotive diesel	45.6	Bagasse	9.6

2.2 Fuel cell

There are various types of fuel cells, and they differ their electrolyte, operating temperature, and ion conduction material.

Table 2.2-1 different types of Fuel cells [11]

Fuel Cell Type	Mobile ion	Operating temperature	Applications
Alkaline (AFC)	OH^-	50-200°C	Used in space vehicles, e.g. Apollo, Shuttle.
Proton Exchange Membrane (PEMFC)	H^+	20-90°C	Vehicles and mobile applications, and for lower power CHP systems
Direct Methanol (DMFC)	H^+	20-90°C	Suitable for portable electronic systems of low power, running for long times
Phosphoric acid (PAFC)	H^+	~220°C	Large number of 200-kW CHP systems in use
Molten Carbonate (MCFC)	CO_3^{2-}	~650°C	Suitable for medium –to large scale- CHP systems, up to MW capacity
Solid oxide (SOFC)	O^{2-}	500-1000°C	Suitable for all sizes of CHP systems, 2kW to multi-MW

Due to the high volumetric power density, start at room temperature, high current density, prompt response, high stability, and a long lifespan, PEMFC is the best solution.

PEMFC has the following reactions [11]:

Anode : $H_2 (g) \rightarrow 2H^+ (aq) + 2e^-$

Cathode : $\frac{1}{2}O_2 (g) + 2H^+ (aq) + 2e^- \rightarrow H_2O (l)$

Overall : $H_2 (g) + \frac{1}{2} O_2 (g) \rightarrow H_2O (l)$ + electric energy + waste heat

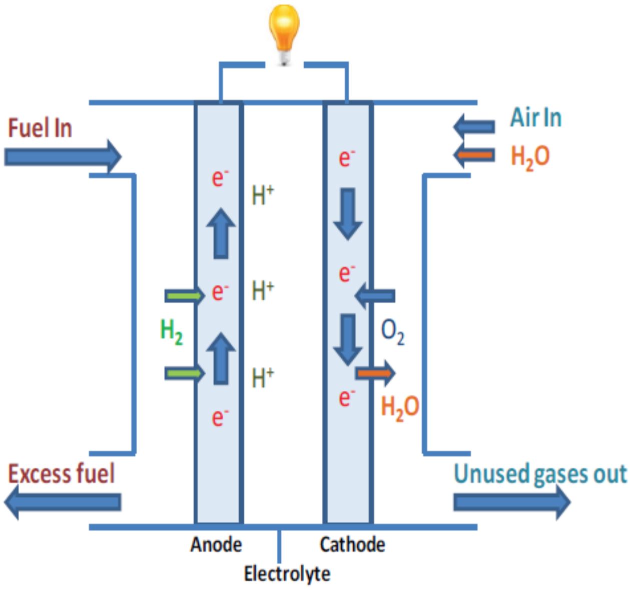

Figure 2.2-1 Operation of PEMFC [11]

2.3 Electrolyzer

Electrolyzer is a equipment which used to generate H_2 gas by using electricity and water.

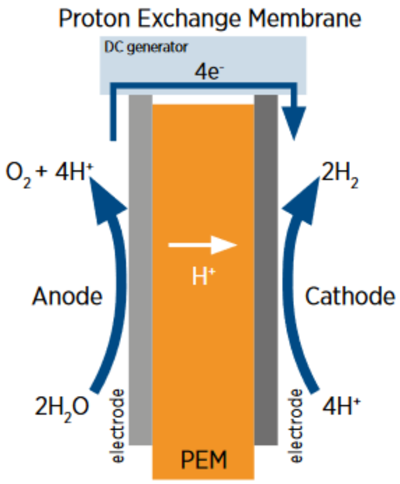

Figure 2.3-1 Operation of Electrolyzer [11]

Electrolyzer has the following reactions [11]:

Anode: $2H_2O \leftrightarrow O_2 + 4H^+ + 4e^-$

Cathode: $4H^+ + 4e^- \leftrightarrow 2H_2$

Table 2.3-1 different types of Electrolyzers [11]

	Alkaline	PEM	AEM	Solid Oxide
Operating temperature	70-90 °C	50-80 °C	40-60 °C	700-850 °C
Operating pressure	1-30 bar	< 70 bar	< 35 bar	1 bar
Electrolyte	Potassium hydroxide (KOH) 5-7 $molL^{-1}$	PFSA membranes	DVB polymer support with KOH or NaHCO3 $1molL^{-1}$	Yttria-stabilized Zirconia (YSZ)
Separator	ZrO_2 stabilized with PPS mesh	Solid electrolyte (above)	Solid electrolyte (above)	Solid electrolyte (above)
Electrode / catalyst (oxygen side)	Nickel coated perforated stainless steel	Iridium oxide	High surface area Nickel or NiFeCo alloys	Perovskite-type (*e.g.* LSCF, LSM)
Electrode / catalyst (hydrogen side)	Nickel coated perforated stainless steel	Platinum nanoparticles on carbon black	High surface area nickel	Ni/YSZ
Porous transport layer anode	Nickel mesh (not always present)	Platinum coated sintered porous titanium	Nickel foam	Coarse Nickel-mesh or foam
Porous transport layer cathode	Nickel mesh	Sintered porous titanium or carbon cloth	Nickel foam or carbon Cloth	None
Bipolar plate anode	Nickel-coated stainless steel	Platinum-coated titanium	Nickel-coated stainless steel	None
Bipolar plate cathode	Nickel-coated stainless steel	Gold-coated titanium	Nickel-coated Stainless steel	Cobalt-coated stainless steel
Frames and sealing	PSU, PTFE, EPDM	PTFE, PSU, ETFE	PTFE, Silicon	Ceramic glass

2.4 General information of telecommunications systems

In the Sri Lankan context, telecommunications systems require a 48V DC power source in general. The system must have an uninterruptible power source at all times due to the nature of the business.

The network locations in execution are layered into three, based on network design and the significance of each site to the overall stability of network which are Core, Aggregation, and Access. The power system's needed backup mechanism and backup capacity for a site are determined by the above-mentioned layer into which the site is classified [3].

The size of the required battery bank and the decision to deploy a diesel generator are governed by the parameters listed above.

There are two main reasons for moving toward solar energy gathering for base station sites:

- Cost reduction
- Moving to greener options as part of corporate social responsibility.

As a result, solar power is typically employed for locations in the access layer, which are less important than those in the other two layers. Prior to making any investment decision, the parameters to evaluate in cost terms will be the optimization of both operational and capital expenditure. As a result, there is no difference in the decision to invest in a solar energy system for electricity generation. As a result of the solar energy harvesting system's configuration, consists of diesel generator and battery bank, the expense of execution is relatively elevating. The regular replacement of batteries and regular maintenance of the generator are the causes to this high expense. When considering solar PV-powered sites, DAP is not altering the size of generator for each site. The standard practice of DAP was to install a diesel generator which rated as 10 kVA, regardless of adjusting any other characteristics. Furthermore, due to storage constraints, the greatest feasible exploitation of available solar energy is not achieved. As a result, when the cost is weighed against the alternatives, the likelihood of a solid business case is minimal.

With the steep rise of electrical energy tariffs, operative companies are looking for alternatives to expand the of solar energy harvest which use to energize base station installations [3].

3. DATA ANALYSE

3.1 Network of the telecommunication

A telecommunication network's base station sites differ from one another. The contrast could be caused by the cooling technique, power load available arrival range (for the purposes of this investigation, solar), and so on. For this study, the Exchange Axiata PLC system was used as the test space of destinations, with the control stack and the arrive region available inside each of the localities for the purpose of data analysis. These details were gleaned from the internal databases of operator. The nuanced characteristics of off-grid destinations, as well as the control supply plan for those, were given a special focus [3].

3.2 Data gathering

There are different strategies for energy storing gathered through a solar energy framework within the industry.

3.2.1 Battery system

One of the most popular procedures in the sector, particularly in the telecommunications industry, is to integrate batteries into the system for the aforementioned reason. The battery bank is designed with batteries those are selected relying on their specializations, limitations of the intended use in addition to obtain module sullied the decision [3].

3.2.2 Hydrogen system

One of the non-traditional notions is storing energy in the form of hydrogen, which has substantial advantages over other solutions. There are still negative effects that must be monitored based on the requirements in order to develop the best ways possible for the purpose.

3.3 Gathered data analysis

The sample size of the acquired information is a critical aspect in determining the feasibility of the suggested concept in real-world circumstances. There are five mobile telecommunications companies on the island, each with a network that stretches virtually the whole length of the island. To test the capability of the planned approach, Dialog Axiata PLC (DAP)'s network is chosen which is Sri Lanka's major mobile operator with the largest number of base station sites.

DAP's network includes of 3039 base station site locations scattered throughout all of Sri Lanka's administrative districts. 54 off-grid sites are there to power up the operations locally. Out of the 54 off-grid facilities, 41 are powered by full-time diesel generators with battery banks on site to ensure an uninterruptible power supply in the event of a generator failure or maintenance shutdown.

The remaining 13 off-grid locations are predominantly powered by solar PV, with backup diesel engines and batteries to employ when insolation is minimum or less accessible [3].

3.3.1 Site categorization

When a site's power requirement is assessed in conjunction with the network, the range is from 0.2 kW to 8 kW. The entire test space was divided into four groups depending on the demanded load in 1 kW increments in order to verify the feasibility of the suggested solution.

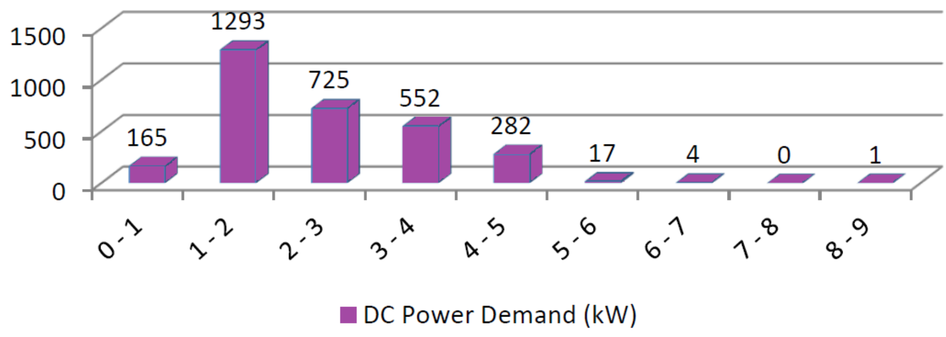

Figure 3.3.1-1 Site count vs the DC demand [3]

Not only the control request, but also the zone accessible inside the site grounds, must be taken into account in order to select the maximum harvest of the power that comes from on-site solar system [3].

3.3.2 Site categorization re-arrangement

The available land space at a site often changes from 300 m^2 to 1000 m^2 over the course of a run. The over segregation in Figure 3.3.1-1 was re-segregated into three ranges for simplicity of analysis and to increase the importance when the commonsense scenario is taken into account.

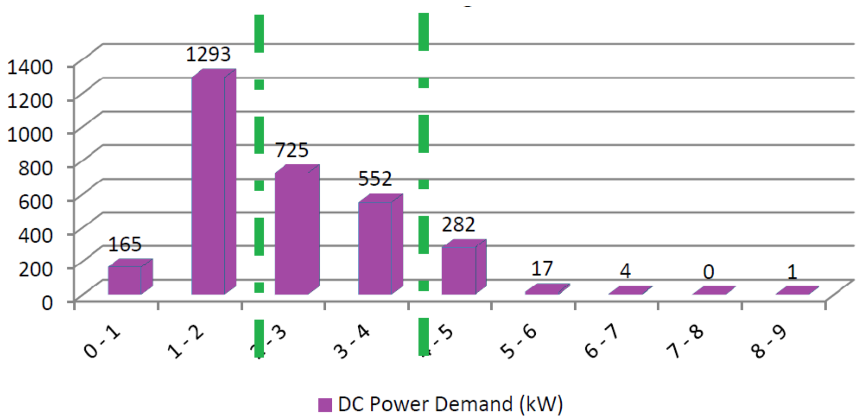

Figure 3.3.2-1 Re-arrange of power demand to take in information on availability of area [3]

Based on the aforementioned segregation indicated in Figure 3.3.2-1, the area available inside the sites was calculated individually for each of the three categories of sites [3].

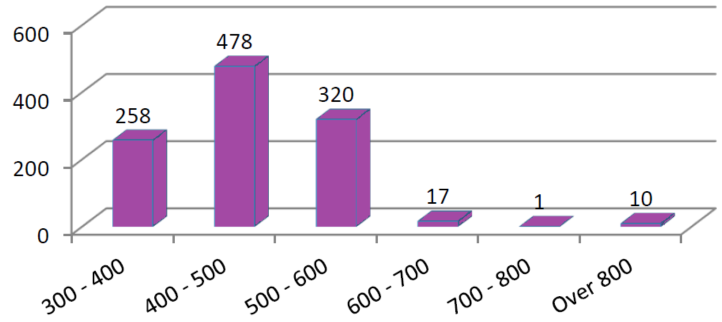

Figure 3.3.2-2 Spread of available site ares with the demand less than 2 kW[3]

The number of sites that fit into each category are shown in Figure 3.3.2-2. The graph is plotted with the information on land areas available inside the sites with less than 2kW power requirement. Figures 3.3.2-3 and 3.3.2-4, respectively, indicate the distribution of areas for remaining two types of power requirement which are 2 kW to 4 kW and over 4 kW.

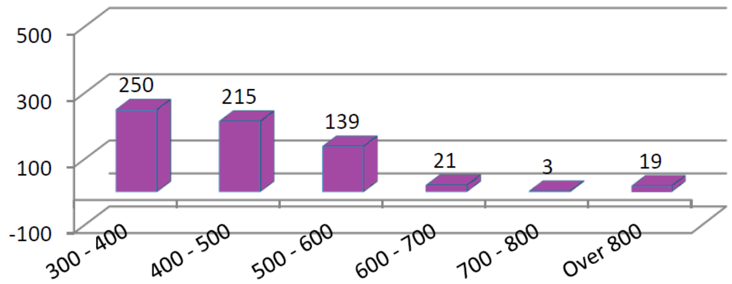

Figure 3.3.2-3 Spread of available site areas with demand between 2 kW – 4 kW[3]

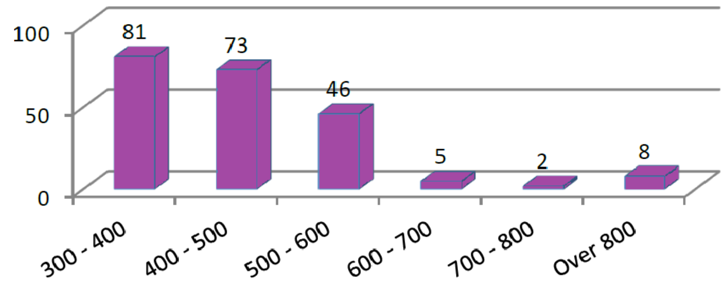

Figure 3.3.2-4 Spread of available site areas with demand greater than 4 kW[3]

The main data collection is extricated from the network has practically accomplished with the above segregation. Typically, because of the fundamental approval of the arrangement's reasonableness in light of local control requirements and the possibility of achieving the similar in practical using a solar photovoltaics panel system [3].

4 MODELLING THE SYSTEM

4.1 PEMFC Power System

In this study, a model of a FC power generation system includes solar PV, electrolyzer, FC, and H_2 storage tank components to simulate the entire operating processes of hydrogen creation, H_2 storage, H_2 utilization, and the electricity production. Figure 4.1-1 depicts the block diagram. The PEMFC model is next investigated via simulation under the premise of an ideal gas state [4].

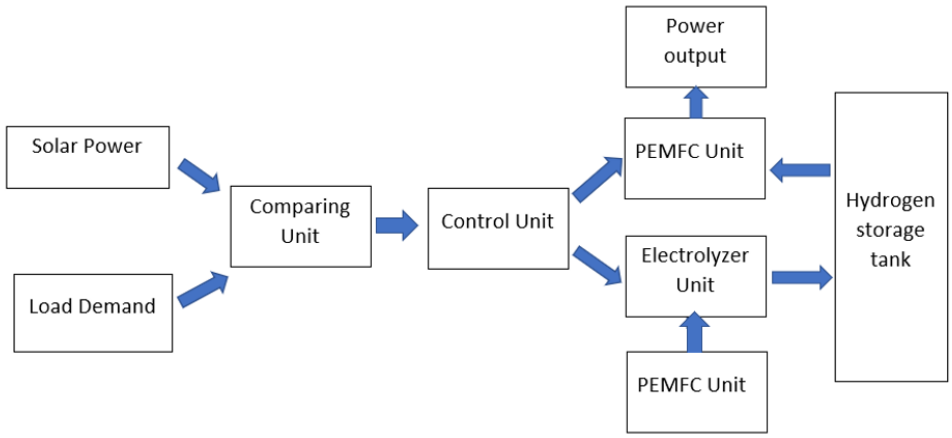

Figure 4.1-1 The Block Diagram for PEMFC System [4]

4.2 Model of mathematical

Figure 4.2-1 depicts the connection of the units of the process of the PEMFC system [4].

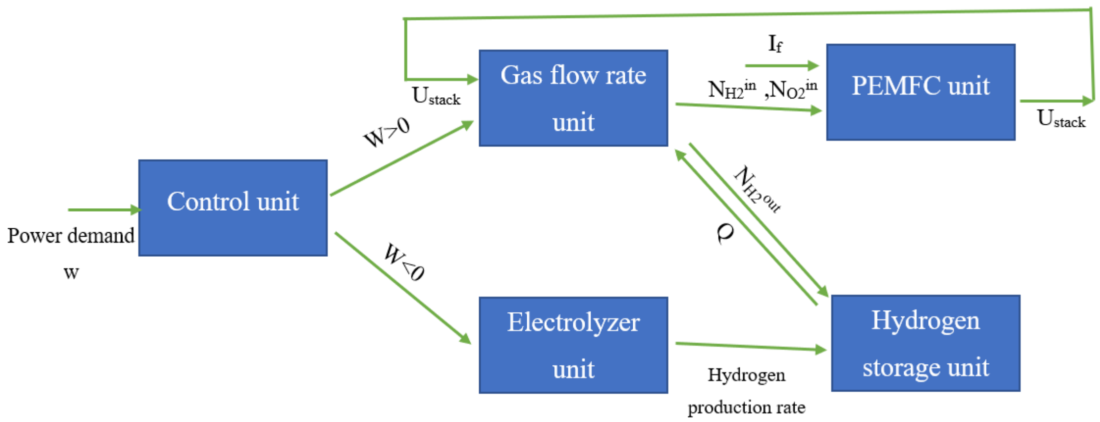

Figure 0-1 The Diagram of Unit Connection in PEMFC System

4.3 Gas Flow Rate Control Unit Model

The equation for the ideal gas state [4]:

$$PV = N\mathrm{R}T$$

P – pressure, Pa

V – gas volume, m^3

N – substance gas amount, mol

R – universal gas constant, 8.314 J/ (mol. K)

T – temp., K.

The material balance equation can be written:

$$\frac{PV}{\mathrm{R}T}\frac{dx_i}{dt} = N_i^{\mathrm{in}} - N_i^{\mathrm{out}} - N_i^{\mathrm{r}}$$

In the case of a FC, partial differential equations can be expressed as follows [4]:

$$\frac{dP_{\mathrm{O_2}}}{dt} = \frac{\mathrm{R}T}{V_{\mathrm{ca}}}(N_{\mathrm{O_2}}^{\mathrm{in}} - N_{\mathrm{O_2}}^{\mathrm{out}} - N_{\mathrm{O_2}}^{\mathrm{r}})$$

$$\frac{dP_{\mathrm{H_2}}}{dt} = \frac{\mathrm{R}T}{V_{\mathrm{a}}}(N_{\mathrm{H_2}}^{\mathrm{in}} - N_{\mathrm{H_2}}^{\mathrm{out}} - N_{\mathrm{H_2}}^{\mathrm{r}})$$

P_{H2} – partial pressure of H_2

P_{02} – partial pressure of O_2

N_{H2}^{in} – mol flow rate of import of H_2

N_{H2}^{out} – mol flow rate of export of H_2

N_{H2}^{r} – mol flow rate of reaction of H_2

N_{02}^{in} – mol flow rate of import of O_2

N_{02}^{out} – mol flow rate of export of O_2

N_{02}^{r} – mol flow rate of reaction of O_2

V_a – FC anode volume

V_{ca} – FC cathode volume

$$PV = NRT, \rho = \frac{m}{v}, N = \frac{m}{M}$$

$$\frac{\rho}{M} = \frac{P}{RT}$$

$$N_{H_2}^{in} = \frac{\rho_{H_2}}{M} Q = \frac{P_g}{RT} Q$$

The PID controller controls the storage tank's valve opening in order to control the N_{H2}^{in} and N_{02}^{in} import flow rates [4].

m – mass in kilograms

M - the mole mass of H_2 in kg mol^{-1}

ρ_{H2} - the H_2 density of H_2 storage tank in kg m^{-3}

Q – open of the valve in H_2 tank in m^3 s^{-1}

P_g – pressure of the H_2 tank

T – temp. of H_2 storage tank.

Output flow rate can be expressed as follows [4]:

$$N_{H_2}^{out} = K_{H_2} P_{H_2}$$
$$N_{O_2}^{out} = K_{O_2} P_{O_2}$$

K_{H2} - valve mole constant of H_2 (4.22 x 10^{-5} kmol/atm.s)

K_{02} - valve mole constant of O_2 (2.11 x 10^{-5} kmol/atm.s)

The flow rate of consumption of reaction [4]:

$$N_{H_2}^{r} = \frac{n}{2F} I_f$$

$$N_{O_2}^{r} = \frac{n}{4F} I_f$$

n - series no. of FC units (80)

F - Faraday constant (96485 C/mol)

I_f - FC operating current, A.

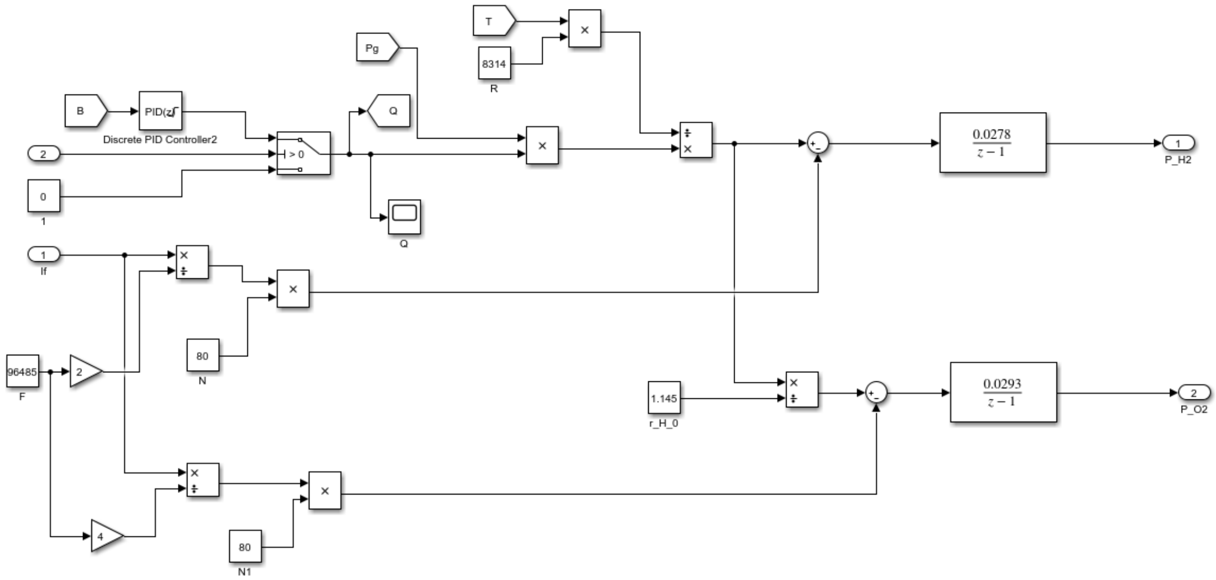

Figure 4.3-1 Model of Gas Flow Rate Unit

4.4 FC modelling using Matlab Simulink

The two techniques of power generation have a hypothetical reversible electrical potential, but because loss of energy is deemed irreversible, the voltage output of the system is smaller than the reversible voltage output. Actuation polarization voltage loss, ohms polarization voltage loss, and concentration polarization voltage loss are among the irreversible losses. Within the PEMFC, the phenomena of the double-charge layer exist at the same moment. The FC offers excellent dynamic properties due to a portion of the double-charge layer [4].

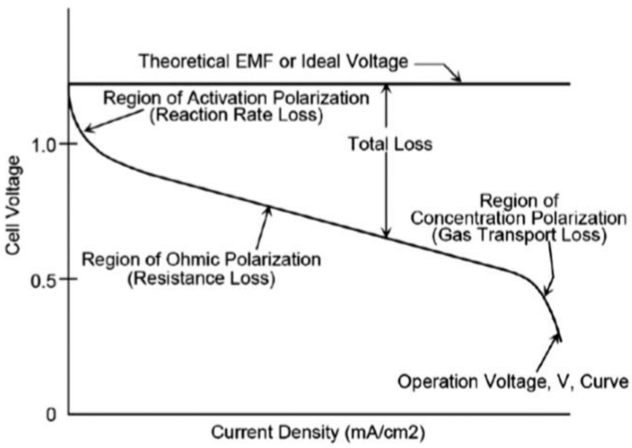

Figure 4.4-1 Fuel cell voltage vs current density

Following that, there are 2 state models of FC voltage output: steady state model and dynamic state model. The voltage output V_c of a single cell is as follows [4]:

Steady model:

$$U_c = U_{nernst} + U_{act} + U_{ohm} + U_{con}$$

Dynamic model:

$$U_c = U_{nernst} + U_{ohm} - U_d$$

V_{nernst} - thermodynamic electromotive voltage

V_{act} - activation polarization loss

V_{ohm} - ohms polarization loss

U_{con} - concentration polarization loss

U_d - equivalent over-loss for dynamic characteristics.

Thermodynamic electromotive voltage [4]:

$$U_{nernst} = 1.229 - 8.5 \times 10^{-4}(T - 298.15) \ + 4.3085 \times 10^{-5} T(\ln P_{H_2} + 0.5 \ln P_{O_2})$$

Activation polarization loss [4]:

$$U_c = -0.9514 + 3.12 \times 10^{-4} T + 7.4 \times 10^{-5} T \ln C_{O_2} - 1.87 \times 10^{-4} T \ln I_f$$

$$C_{O_2} = \frac{P_{O_2}}{5.08 \times 10^{-6} \exp(-498/T)}$$

C_{O2} is the dissolved oxygen concentration at the cathode catalyst contact [4].

Ohms polarization voltage [4]:

$$U_{ohm} = -I_f (Z_m + Z_c)$$

Z_m - impedance of equivalent membrane

Z_c – impedance which prevents protons from passing through the proton membrane (0.0003 Ω)

$$Z_m = \frac{\rho_M l}{A}$$

$$\rho_M = \frac{181.6[1+0.03(I_f/A)+0.062(T/303)^2(I_f/A)^{2.5}]}{[\lambda-0.634-3(I_f/A)]\exp[4.18(T-303)/T]}$$

ρ_M - PEM resistivity, Ω/cm

l - proton membrane’s thickness, cm (0.01 cm)

A - PEM’s activation area (150cm^2)

λ - PEM’s water content (14)

Concentration polarization loss [4]:

$$U_{con} = 0.016 \ln(1-\frac{J}{J_{max}})$$

J - current density of the FC, A cm^{-2}

J_{max} - maximum current density (0.5 - 1.5 A cm^{-2}).

The activation polarization loss and concentration polarization loss effects can be equated to an equivalent resistance R_a and C - parallel capacitance due to the phenomena of the double-charge layer. The fuel cell's corresponding dynamic model can be written as [4]:

$$R_a = -\frac{U_{act}+U_{con}}{I_f}$$

On the dynamic properties, the equivalent polarization over-voltage U_d can be stated as follows [4]:

$$\frac{dU_d}{dt} = \frac{I_f}{C} - \frac{U_d}{CR_a}$$

The voltage output of the FC stack:

$$U_{stack} = nU_c$$

The power output of the FC stack:

$$P_{stack} = U_{stack} I_f$$

Due to electrode polarization losses, internal resistance, and fuel inefficiency, the actual fuel cell power generation efficiency can be written as [4]:

$$\eta_{\mathrm{f}} = \eta_{\max} \frac{U_{\mathrm{c}}}{U_{\mathrm{nernst}}} u_{\mathrm{f}}$$

U_f is the efficiency of the fuel, which ranges from 69 % - 89 %. η_{max} is the potential maximum efficiency of the FC, which is 83 %. When the actual operation of the FC production system is taken into account, as well as the energy consumption of ancillary apparatus such as gas humidifiers, fans, and control equipments, the external output electricity of the FC has an effectual coefficient k, then [4]

$$P_{\mathrm{out}} = kP_{\mathrm{stack}}$$

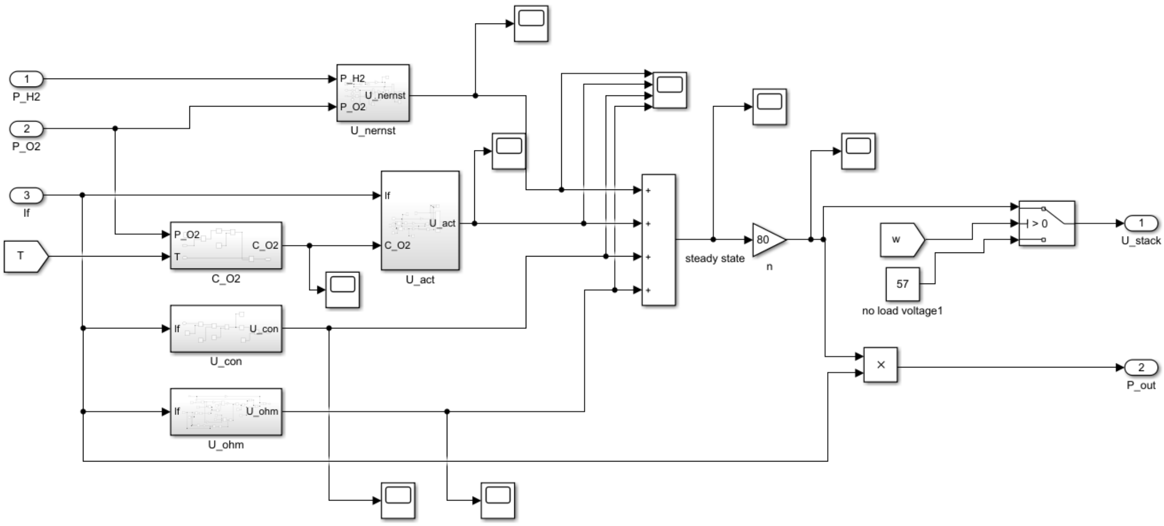

Figure 4.4-2 PEMFC Matlab Simulink model

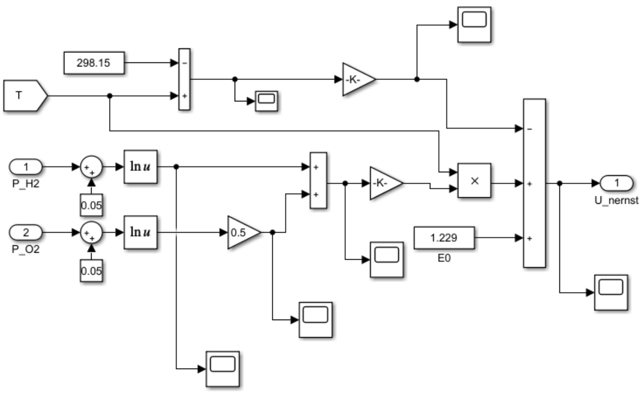

Figure 4.4-3 Matlab Simulink model for U_{nernst}

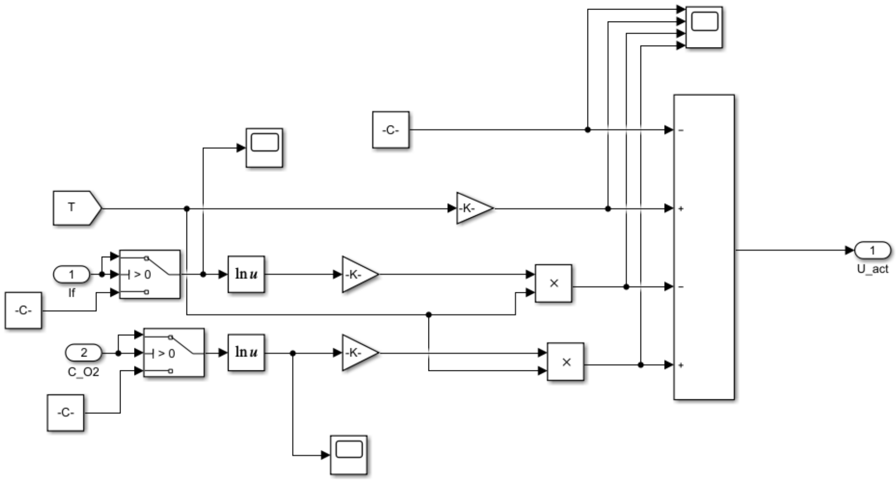

Figure 4.4-4 Matlab Simulink model for U_{act}

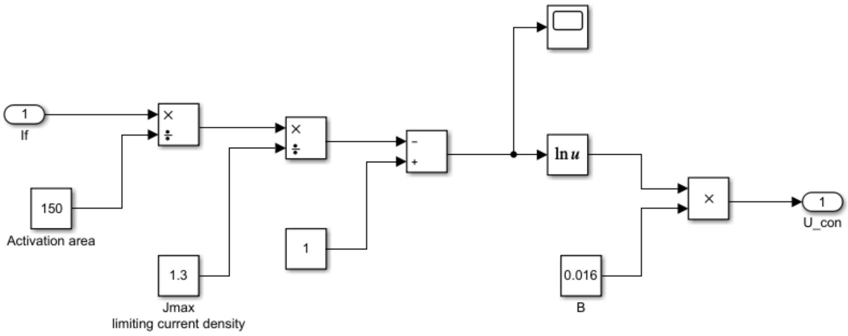

Figure 4.4-5 Matlab Simulink model for U_{con}

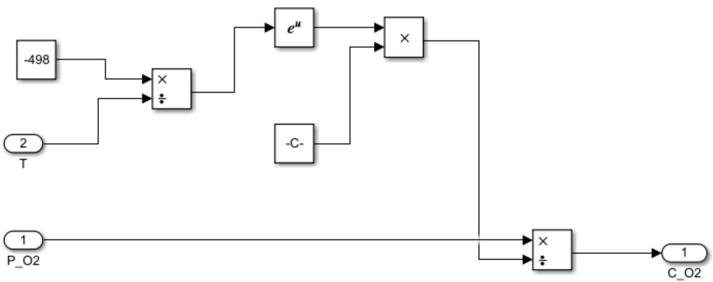

Figure 4.4-6 Matlab Simulink model for concentration of dissolved oxygen

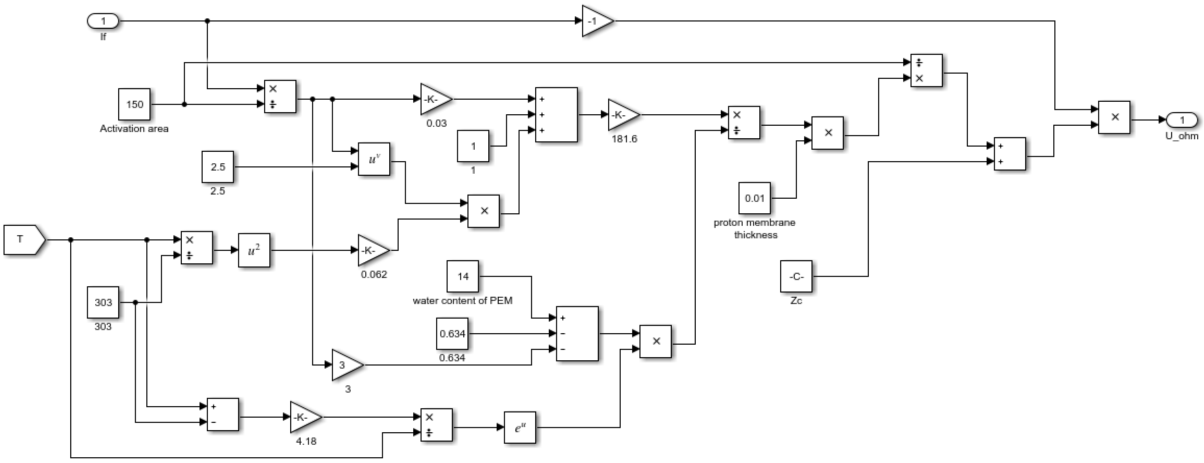

Figure 4.4-7 Matlab Simulink model for U_{ohm}

4.5 Matlab Simulink Model for Electrolyzer

Water electrolysis is the reversal of the power generating process in which H_2O is disintegrated to produce H_2 and O_2 in FC. The of H_2 production rate (mol s^{-1}) is written as [4]:

$$N_{H_2} = \eta_e N_e \frac{I_e}{2F}$$

η_e - electrolysis efficiency of the electrolyzer (60 % - 80 %)

N_e - no. of electrolyzer units in series

I_e – electrolyzer current

Pe - power input of electrolyzer in W

U_e - unit voltage in electrolyzer (1.651V - 2.201V)

$$I_e = \frac{P_e}{N_e U_e}$$

The efficiency of overall conversion of the cycle may then be calculated as follows :

$$\eta_{H_2} = \eta_e \eta_f$$

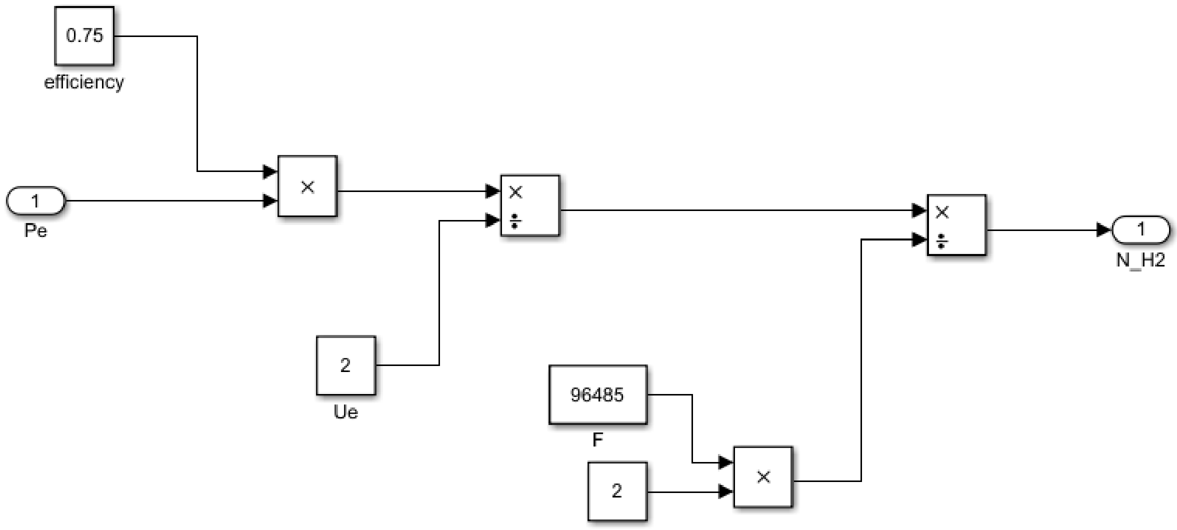

Figure 4.5-1 Electrolyzer Matlab Simulink model

4.6 Matlab Simulink Model for Hydrogen tank

The pressure of the H_2 tank is as follow:

$$P_g = P + \Delta P_1 + \Delta P_2 - \Delta P_3$$

ΔP_1 represents the increase in pressure in the H_2 tank caused by produced H_2 input, Pa; ΔP_2 represents the increase in pressure in the H_2 tank caused by recovering H_2 from FC exports, Pa; and ΔP_3 represents the decrease in pressure in the H_2 tank caused by output H_2, Pa. The equation of ideal gas state can be used to sketch them [4]:

$$\Delta P_1 = \frac{\Delta N_1 \mathrm{RT}}{\mathrm{V}} = \frac{N_{\mathrm{H2}} \mathrm{tRT}}{\mathrm{V}}$$

ΔN_1 - quantity of produced H_2 of the electrolyzer in mol

t – time in s

V - volume of the H_2 storage tank.

$$\Delta P_2 = \frac{\Delta N_2 \mathrm{RT}}{\mathrm{V}} = \frac{k' N_{\mathrm{H2}}^{\mathrm{out}} \mathrm{tRT}}{\mathrm{V}}$$

ΔN2 - quantity of discharged H_2 of FC stack in mol

k' - recovery rate of H_2 (0.9)

$$\Delta P_3 = \frac{Qt}{V} P_g$$

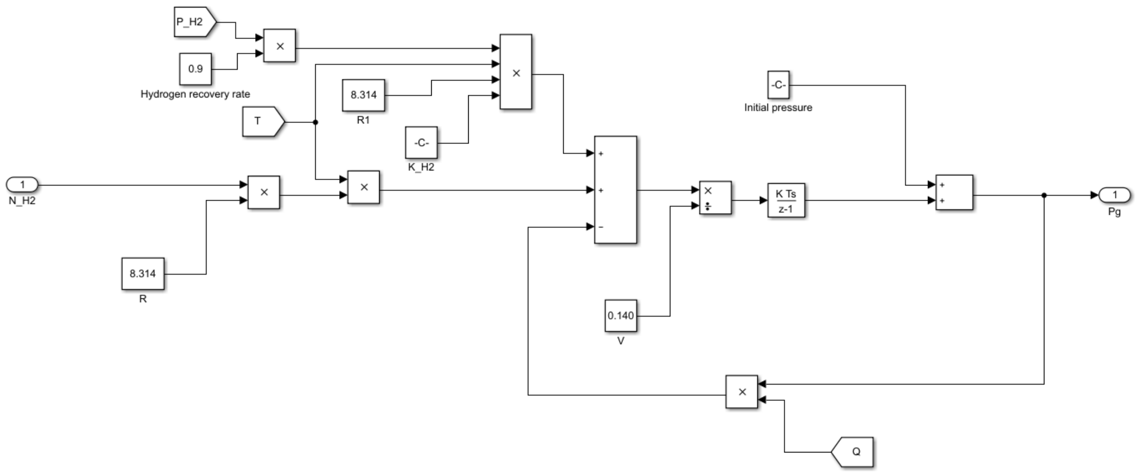

Figure 4.6-1 Hydrogen tank Matlab Simulink model

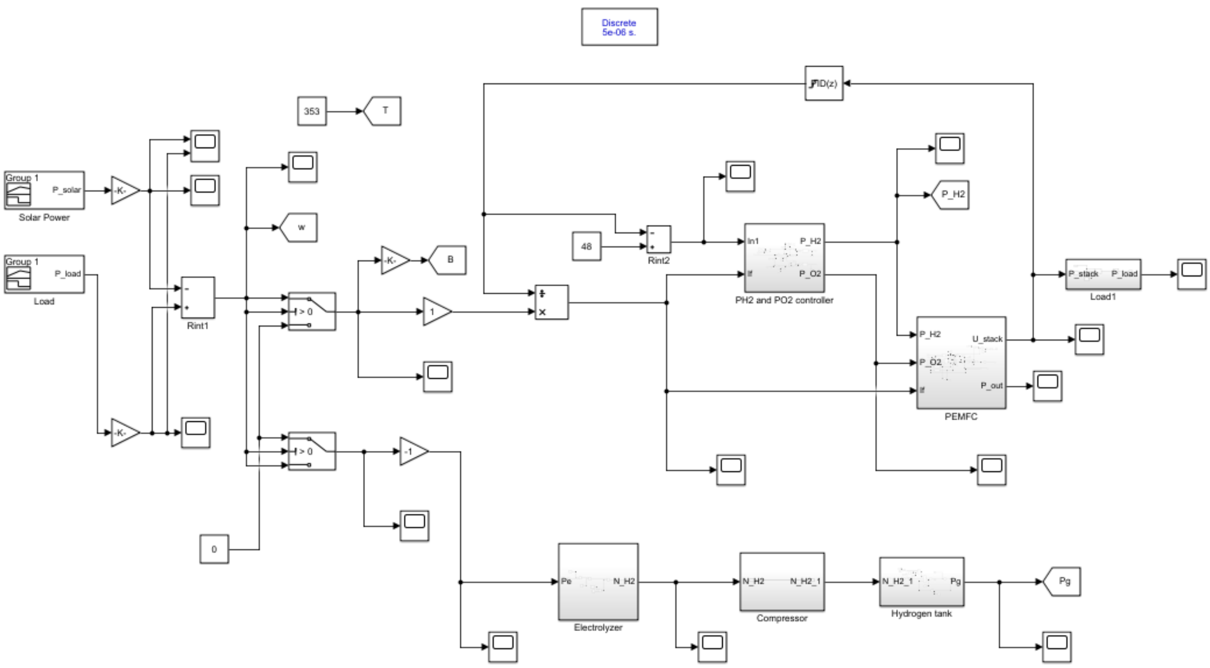

Figure 4.6-2 The Simulation Diagram for the System

4.7 Battery Model

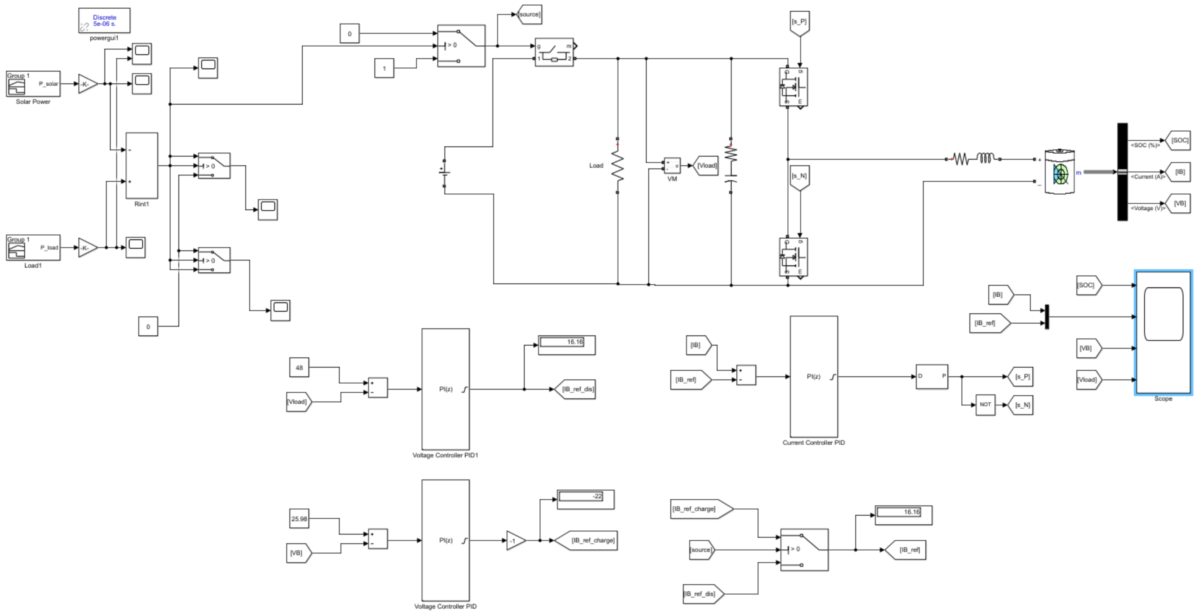

Figure 4.7-1 The Simulation Diagram for battery and the system

5. SIMULATION RESULTS AND ANALYSIS

5.1 1st Test case

Load demand - 0.5 kW

Table 5.1-1 equipments sizes in 1st test case

PV array	2 kW
Fuel cell	2.5 kW
Electrolyzer	2 kW
Hydrogen tank	4.5 kg

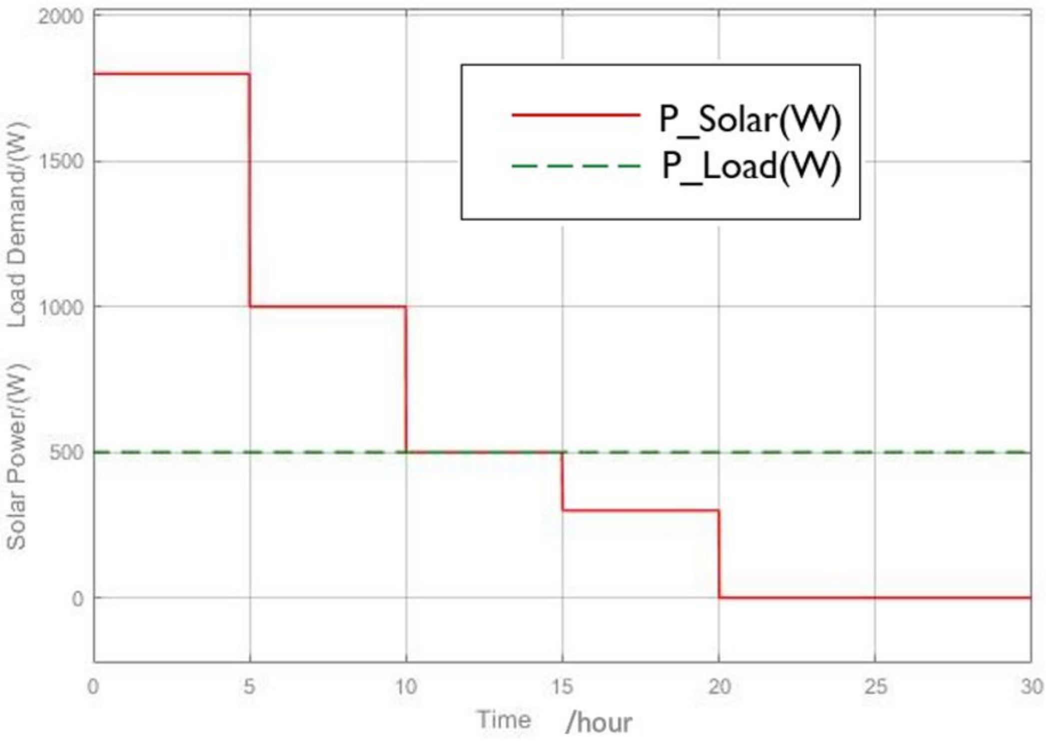

Figure 5.1-1 Solar Power and Load Demand

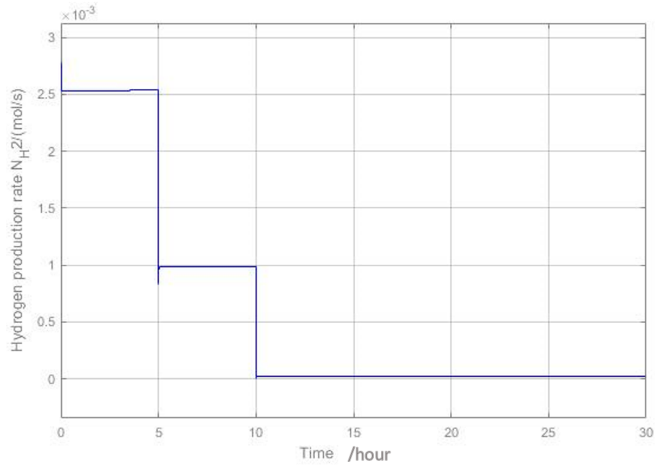

Figure 5.1-2 The variation of H_2 Production in Electrolyzer with the time

Surplus power drives the electrolyzer to create hydrogen in the first 10 hours, as shown in Figure 5.1-2. The excess power decreases from 1300W - 500W in the 5th hour, and the hydrogen production rate drops from 2.5 x 10^{-3} mol/s to 1x 10^{-3} mol/s, and the electrolyzer stops working when there is no surplus power.

When there is a surplus of electricity, the PEMFC operates in standby-mode at no load voltage, as shown in Figure 5.1-3. Electricity shortages occur at the 15th hour. After a short startup time, it reaches its regular operational state and is stable at the default voltage of 48 V. The power requirement changes at the 20th hour, and the voltage of the FC swings before immediately stabilizing at the pre-set value. As a result, the simulation model has a quick response time and can produce a consistent output voltage.

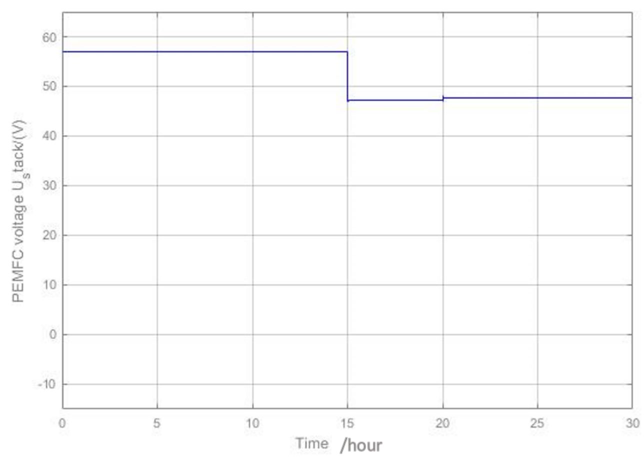

Figure 5.1-3 The output variation of voltage in PEMFC with the time

Figure 5.1-4 shows that the electricity demand varies from 0 to 200 W at the 15th hour, and the current increases rapidly after a small fluctuation at the 20th hour, the power demand changes from 200W to 500W, and the current increases rapidly. Operating current varies in response to changes in electricity demand, has a small fluctuation, and then rapidly returns to a steady state.

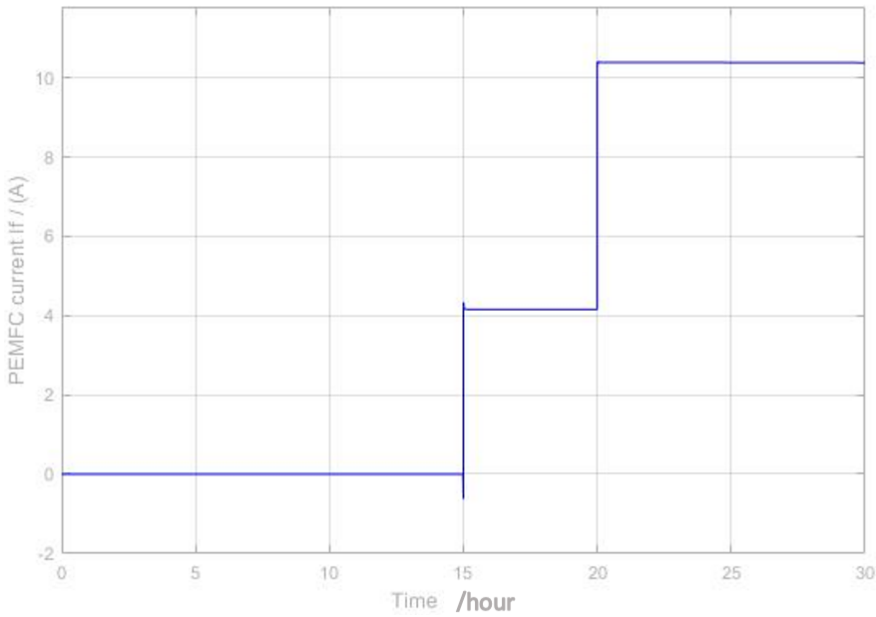

Figure 5.1-4 The output variation of current in PEMFC with the time

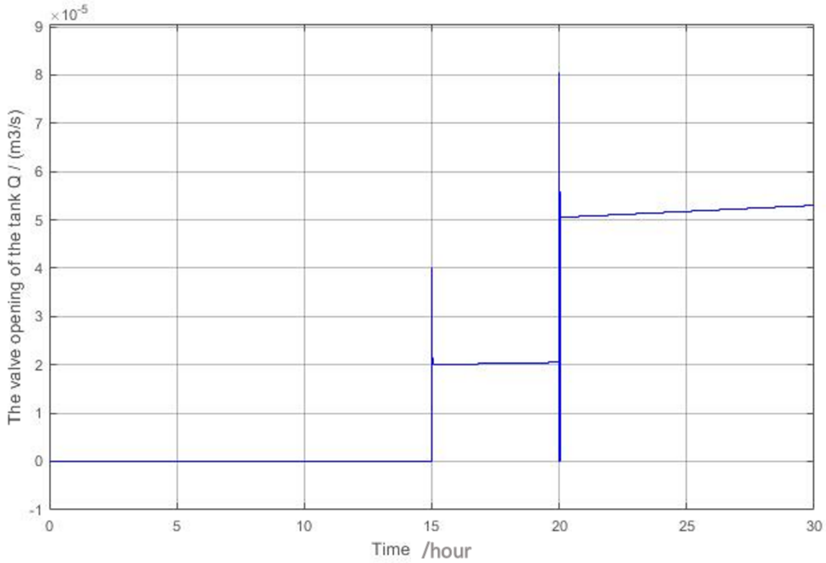

Figure 5.1-5 The output variation of the open in valve in H_2 Tank with the time

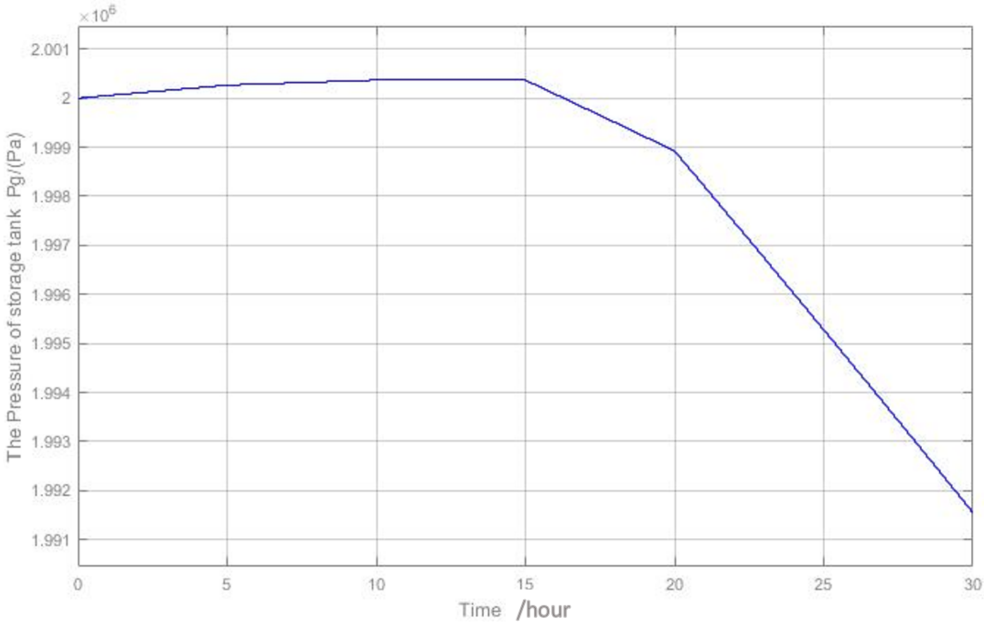

Figure 5.1-6 The output variation of the Pressure in H_2 Tank with the time

The dynamic parameters of a H_2 storage unit are shown in Figures 5.1-5 and 5.1-6. When the power demand varies, the system can response rapidly and have an excellent dynamic behavior. When the entire system's power is surplus, the H_2 tank pressure rises; when the power created falls short of demand, the valve opens wider to generate more power via electro-chemical reaction. As a result, the model is able to track variations in power consumption and is consistent with the actual system.

5.2 2nd Test case

Load demand - 1.5 kW

Table 5.2-1 equipments sizes in 2nd test case

PV array	3 kW
Fuel cell	2.5 kW
Electrolyzer	2 kW
Hydrogen tank	6.5 kg

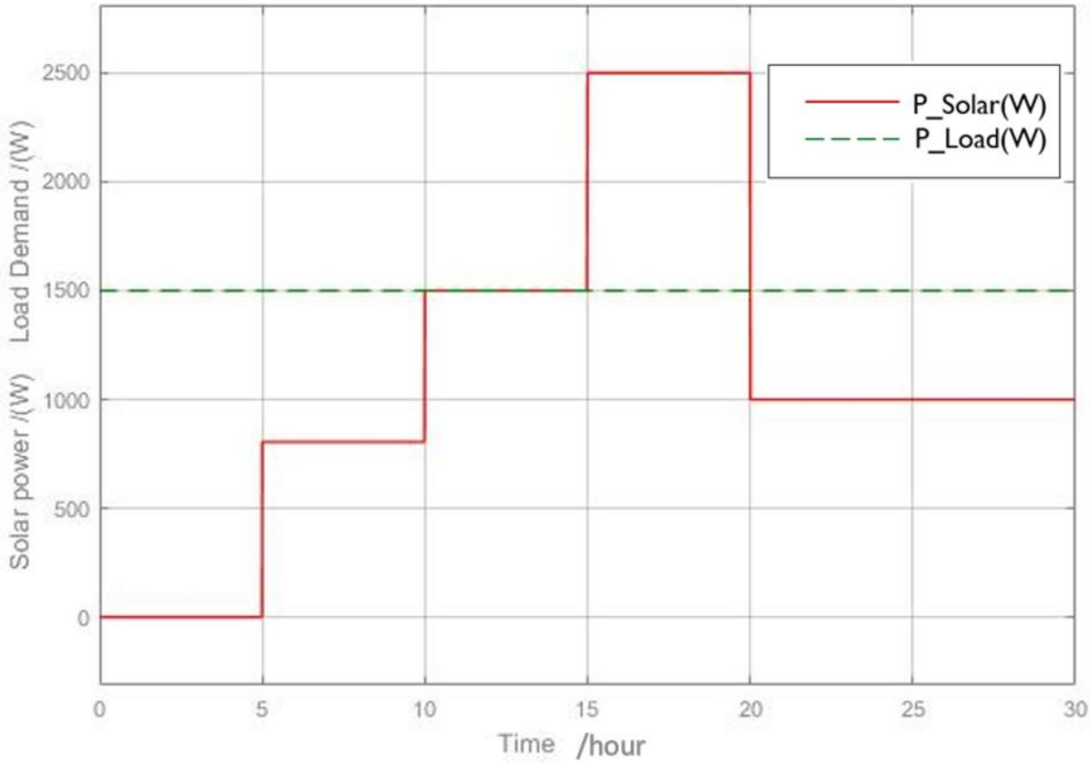

Figure 5.2-1 Solar Power and Load Demand

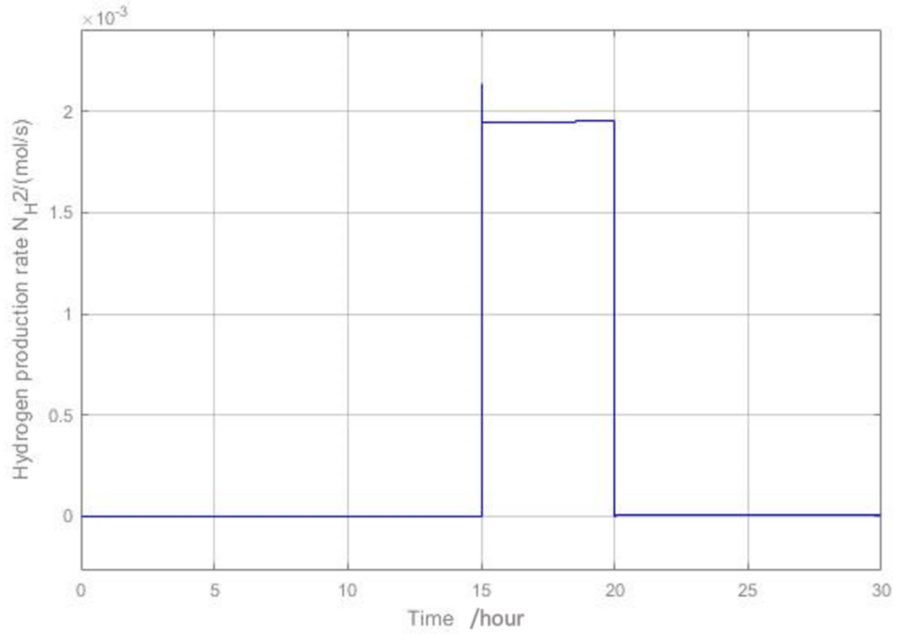

Figure 5.2-2 The output variation of H_2 Production in Electrolyzer with the time

Figure 5.2-2 shows that there is no surplus power in the first 15 hours, thus the electrolyzer is turned off. The surplus power varies from 0 to 1000W at the 15th hour, the electrolyzer starts, and the H_2 production rate increases from 0 to 1.95 x 10^{-3} mol/s. At the 20th hour, the electrolyzer stops working because there is no surplus power.

The PEMFC is in on mode when there is no power surplus, as shown in Figure 5.2-3. Surplus power changed from 1500 W to 700 W at the 5th hour, with the small fluctuation fuel cell voltage stabilizing at 47 V. The surplus power shifted from 700 W to 0 in the 10th hour, and the fuel cell stopped at that point, remaining at no load voltage. When there is a power shortage at the 20th hour, the fuel cell restarts, and after a short startup period, it enters its normal operational state and is stable at the default voltage of 48 V.

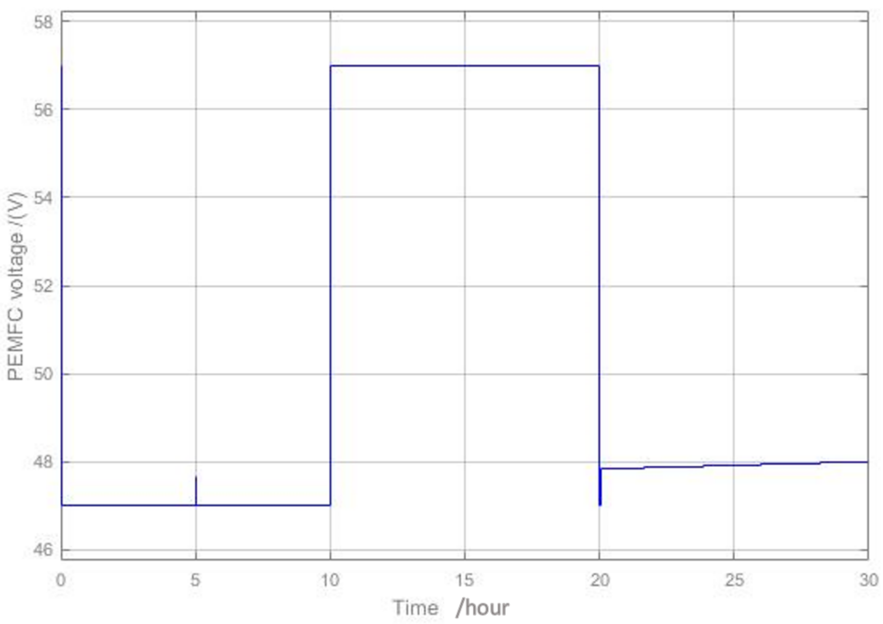

Figure 5.2-3 The output variation of the Voltage in PEMFC with the time

Figure 5.2-4 shows that the power demand reduced at the 5th hour, and the current rapidly decreased; in the 10th hour, the current will be zero because the fuel cell is in the off condition. Operating current varies in response to changes in electricity demand, has a small fluctuation, and then rapidly returns to a steady state. Due to the initiation of the FC, current surged again at the 20th hour.

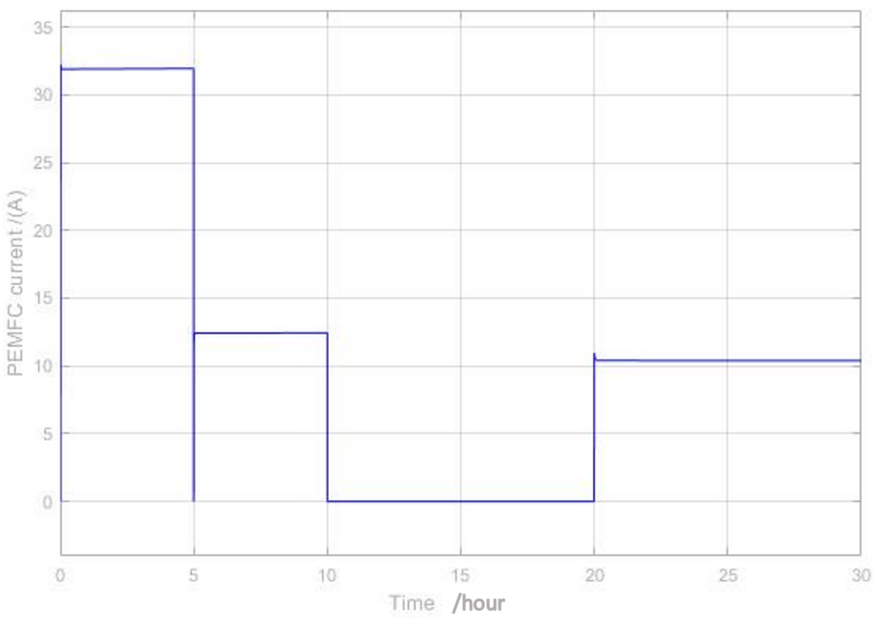

Figure 5.2-4 The output variation of the Current in PEMFC with the time

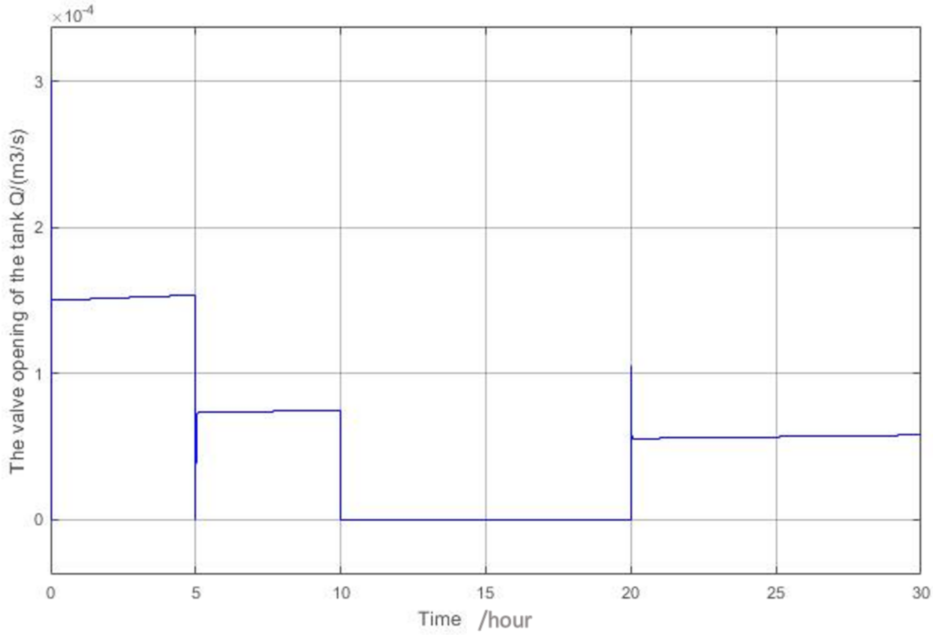

Figure 5.2-5 The output variation of the open of the valve in H_2 Tank with the time

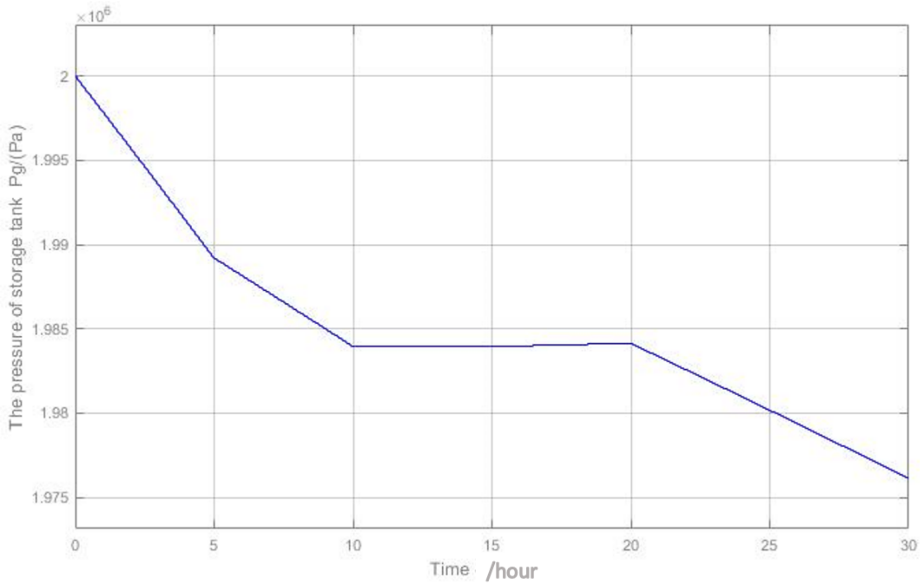

Figure 5.2-6 The output variation of the Pressure in H_2 Tank with the time

The dynamic parameters of H_2 storage unit are shown in Figures 5.2-5 and 5.2-6. When the power demand varies, the system able to respond rapidly and have an excellent dynamic behavior. When there is no power surplus, the H_2 tank pressure drops, while the open of the valve rises, allowing the electrochemical reaction to produce additional power. As a result, the model is able to track variations in power consumption and is consistent with the actual system.

5.3 3rd Test case

Load demand - 1.8 kW

Table 5.3-1 equipments sizes in 3rd test case

PV array	4 kW
Fuel cell	2.5 kW
Electrolyzer	2 kW
Hydrogen tank	8 kg

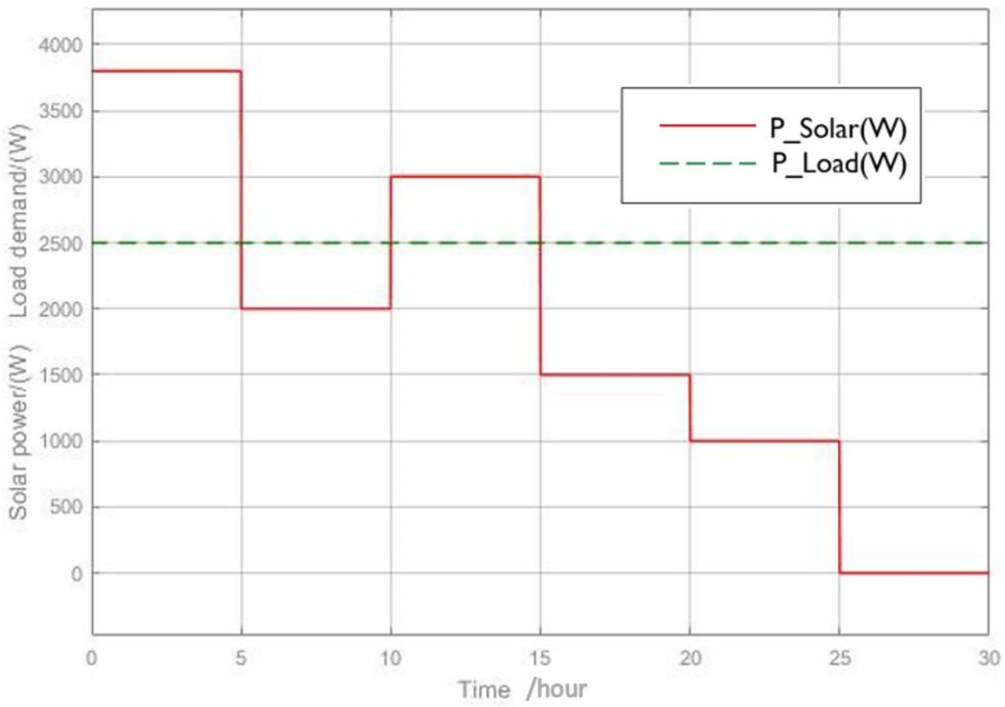

Figure 5.3-1 Solar Power and Load Demand

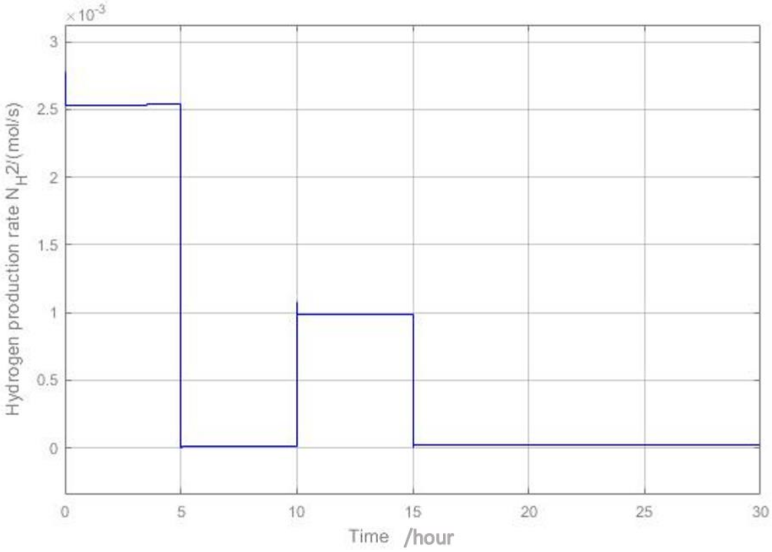

Figure 5.3-2 The output variation of H_2 Production in Electrolyzer with the time

Surplus power drives the electrolyzer to produce H_2 in the first 5 hours, as shown in Figure 5.3-2. The electrolyzer will stop working at the 5th hour due to no surplus power. The electrolyzer will function again in 10–15 hours, and if there is no surplus electricity, it will stop working after the 15th hour.

When there is a surplus of electricity, the PEMFC operates in standby mode at no-load voltage, as shown in Figure 5.3-3. Electricity shortages occur at the fifth hour. After a short startup time, it reaches its regular operational state and is stable at the default voltage of 48 V. At the tenth hour, the fuel cell goes into standby mode, and at the fifteenth hour, it starts up again.

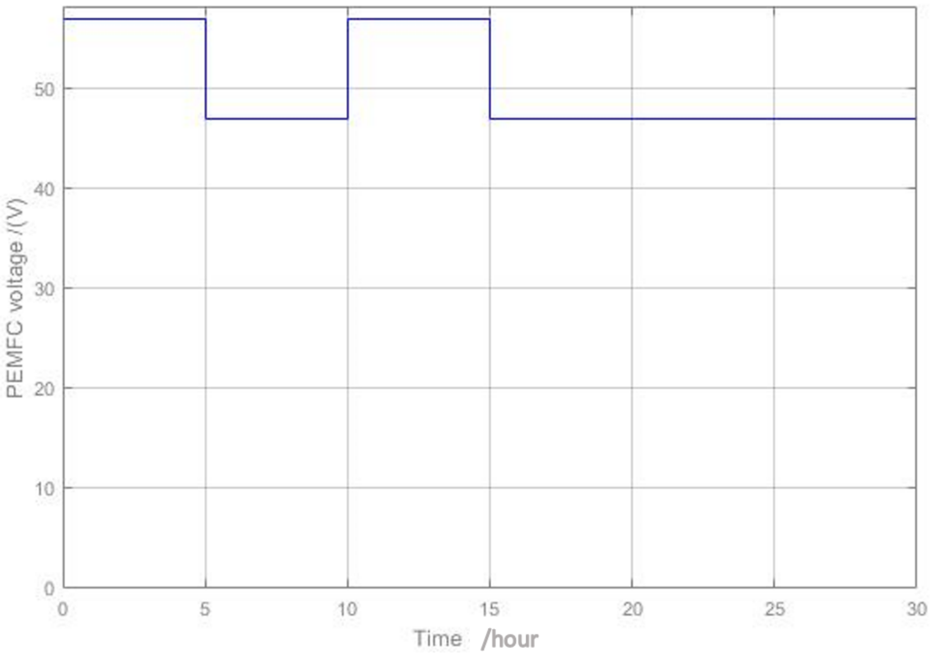

Figure 5.3-3 The output variation of the Voltage in PEMFC with the time

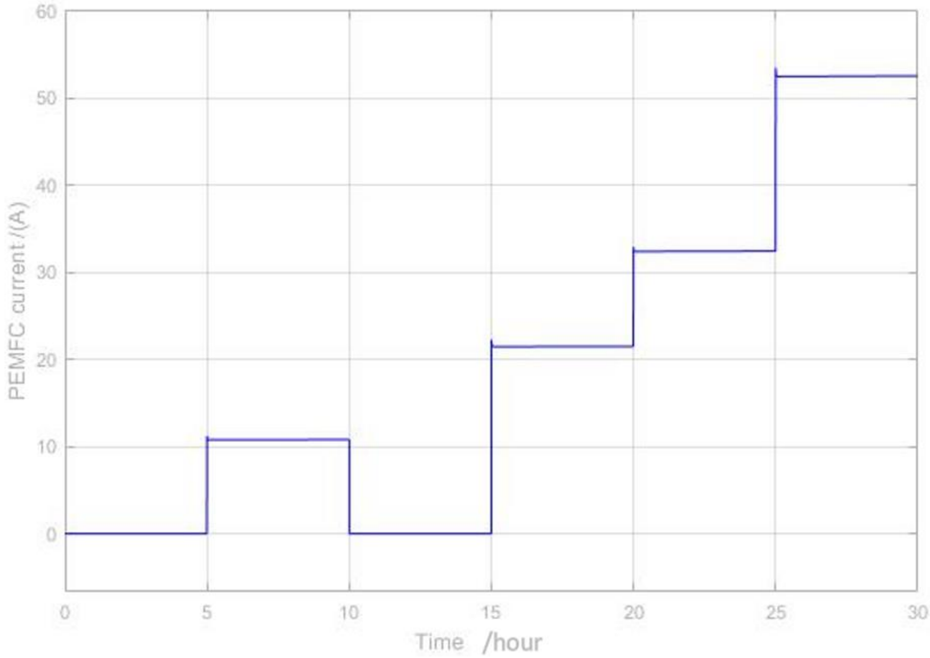

Figure 5.3-4 The output variation of the Current in PEMFC with the time

Accordingly, current of the FC, the open of the valve in H_2 tank and pressure of the H_2 tank will change.

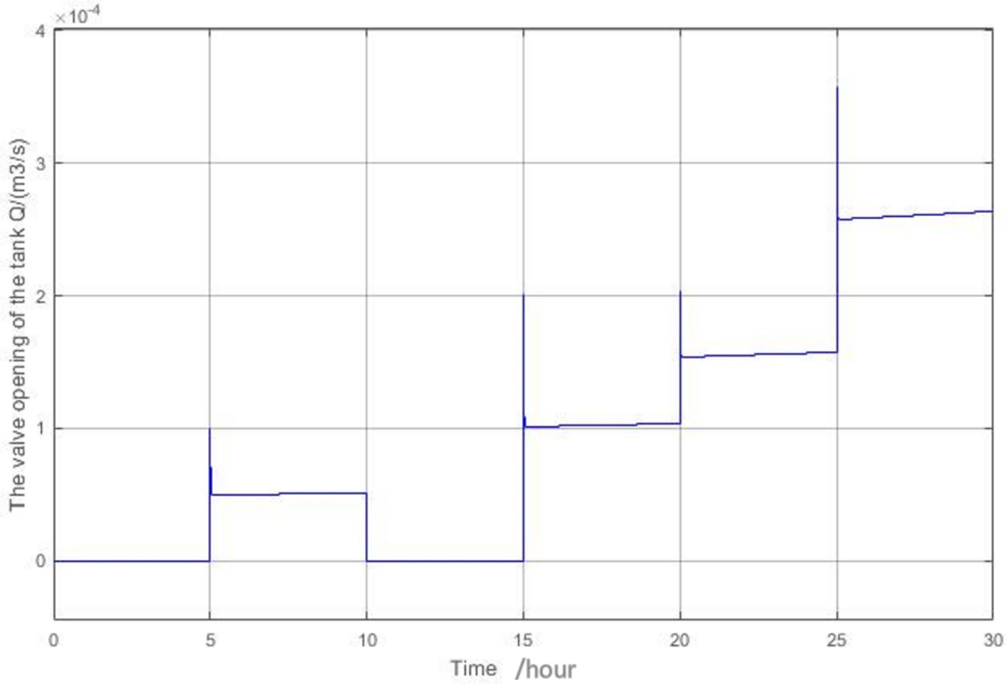

Figure 5.3-5 The output variation of the open of the valve in H_2 Tank with the time

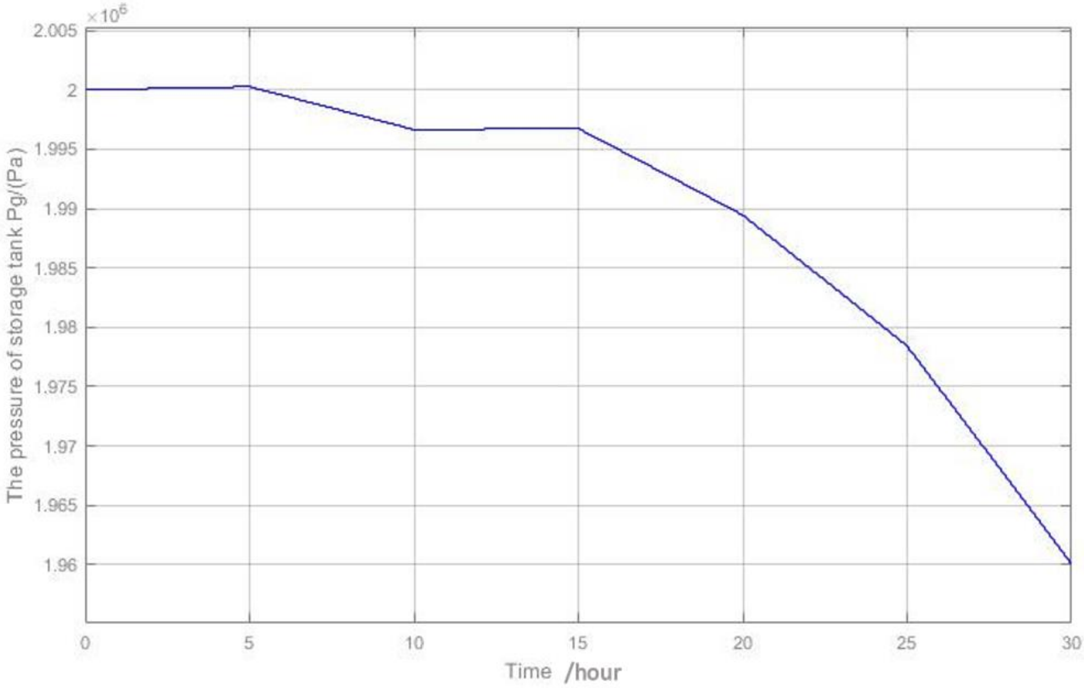

Figure 5.3-6 The output variation of the Pressure in H_2 Tank with the time

5.4 4th Test case

Load demand – 2.5 kW

Table 5.4-1 equipments sizes in 4th test case

PV array	4 kW
Fuel cell	2.5 kW
Electrolyzer	2 kW
Hydrogen tank	9.5 kg

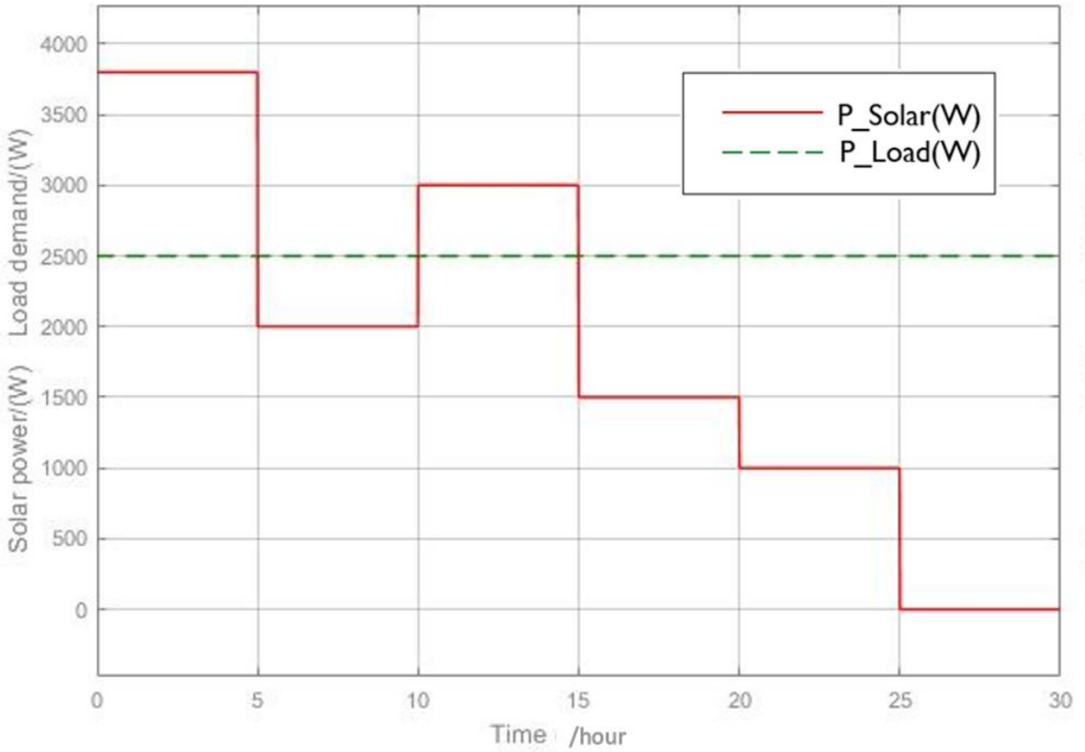

Figure 5.4-1 Solar Power and Load Demand

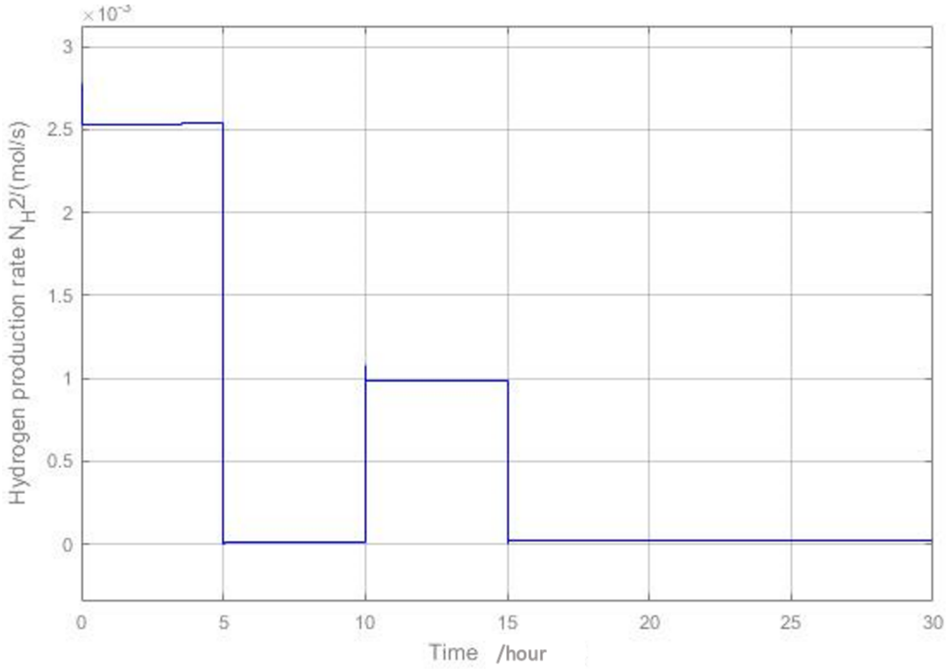

Figure 5.4-2 The output variation of H_2 Production in Electrolyzer with the time

Surplus electricity drives the electrolyzer to create hydrogen in the previous 5 hours, as shown in Figure 5.4-2. The electrolyzer will stop working at the 5th hour if there is no surplus power. The electrolyzer will function again in 10–15 hours, and if there is no surplus electricity, it will stop working after the 15th hour.

The FC is in standby mode at no-load voltage when the electricity is surplus, as shown in Figure 5.4-3. Electricity shortages occur in the 5th hour, and FC resumes normal operation after a small startup period, remaining steady at the preset voltage of 48 V. At the tenth hour, the fuel cell goes into standby mode, and at the fifteenth hour, it starts up again.

Accordingly, FC current, the open of the valve in H_2 tank and the pressure of the H_2 tank will change.

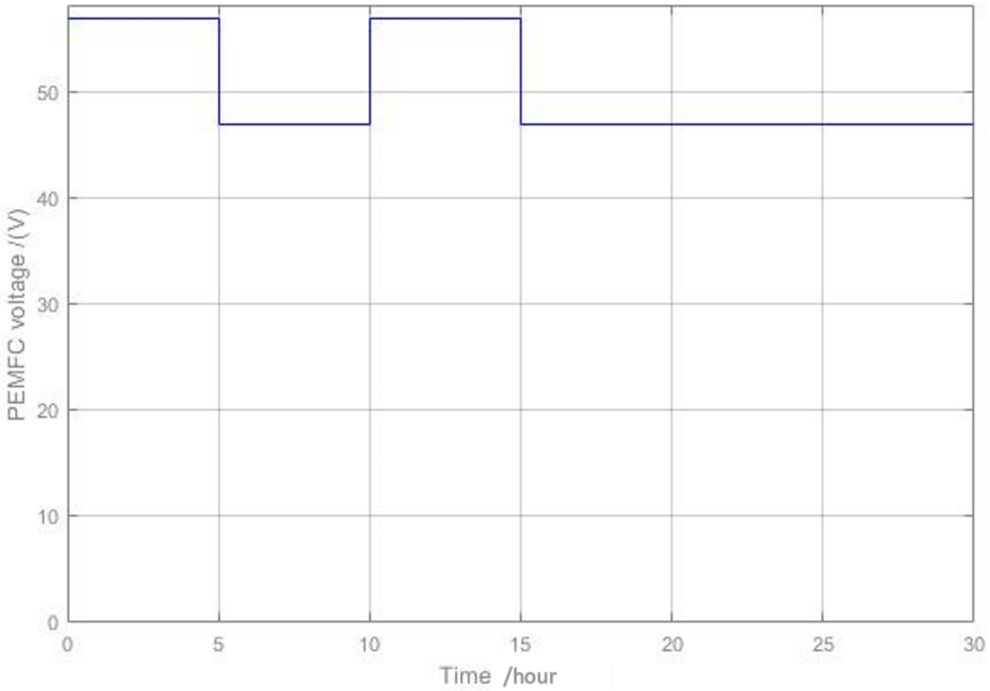

Figure 5.4-3 The output variation of the Voltage in PEMFC with the time

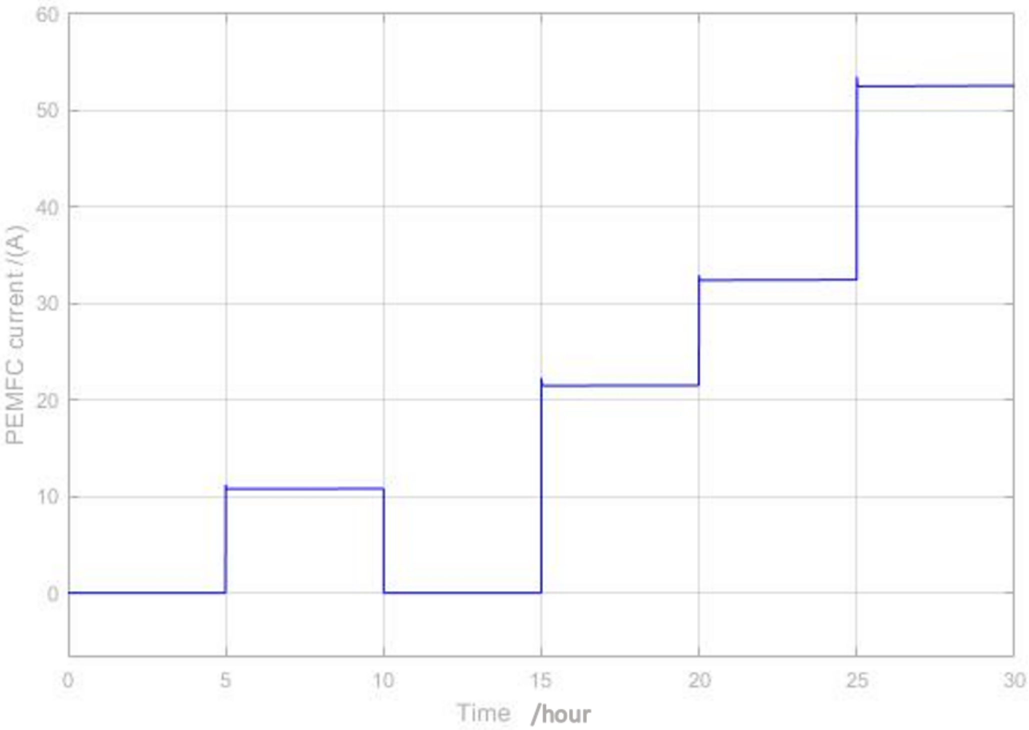

Figure 5.4-4 The output variation of Current in PEMFC with the time

Accordingly, FC current, the open of the valve in H_2 tank and the pressure of the H_2 tank will change.

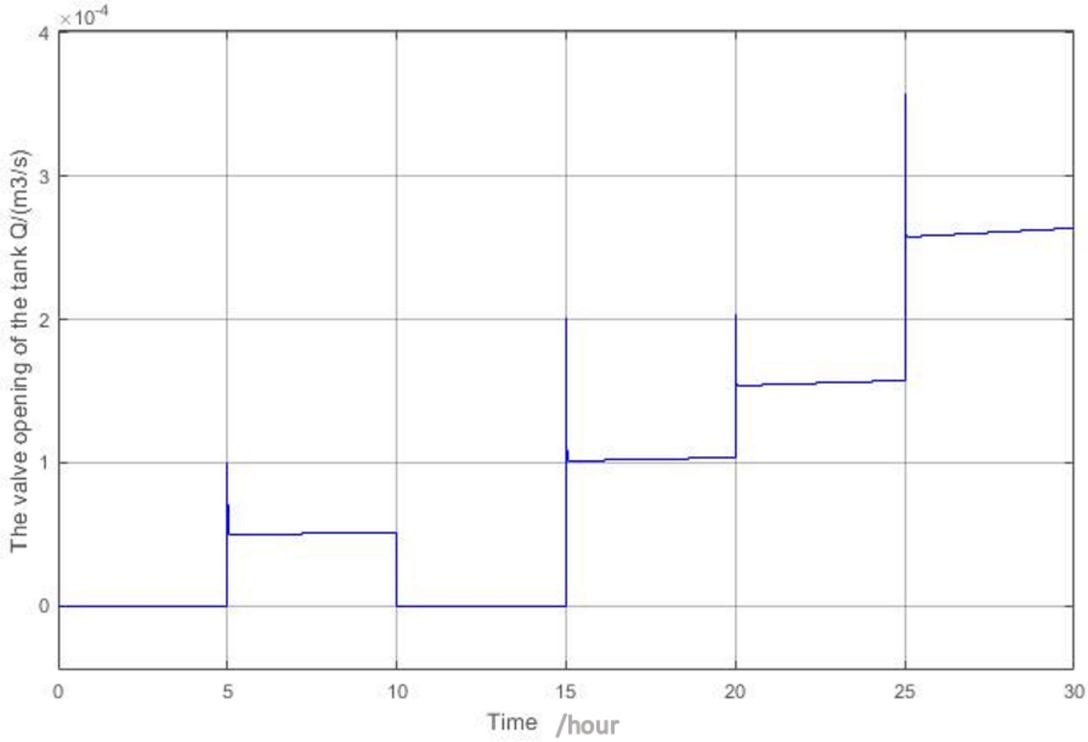

Figure 5.4-5 The output variation of the open of the valve in H_2 Tank with time

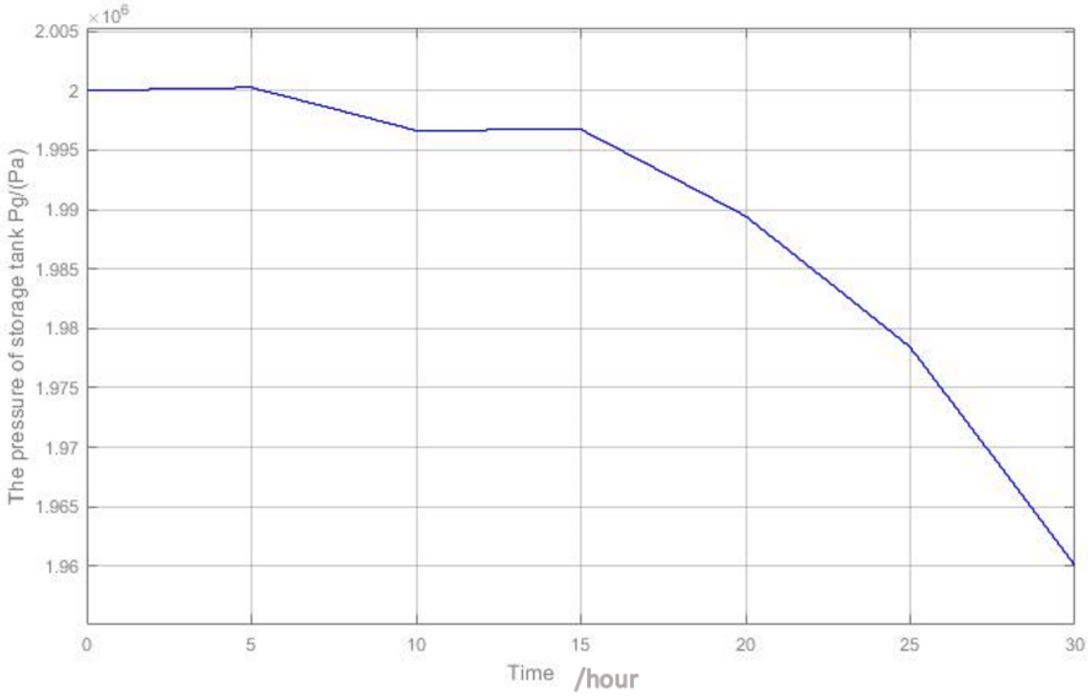

Figure 5.4-6 The output variation of the Pressure in the H_2 Tank with the time

5.5 Analysis for power variation in a day with the hydrogen system

The variation of solar PV production is shown in Figure 5.5-1, and the load variation is assumed to be constant throughout the day.

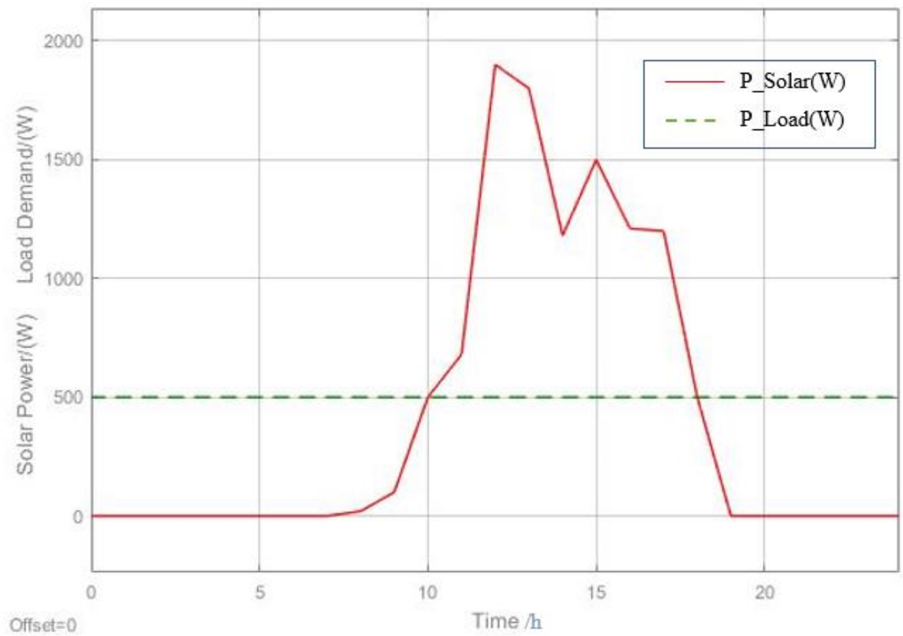

Figure 5.5-1 Solar Power and Load Demand

Figure 5.5-2 shows the output variation of the H_2 produced in electrolyzer.

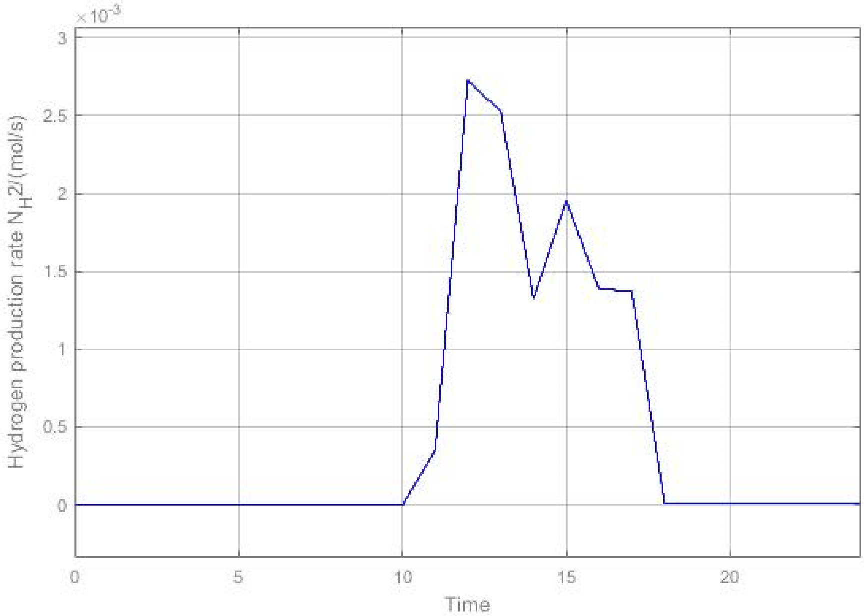

Figure 5.5-2 The output variation of H_2 Production in the Electrolyzer with the time

Figure 5.5-3 shows the output variation of the voltage in PEMFC with the time.

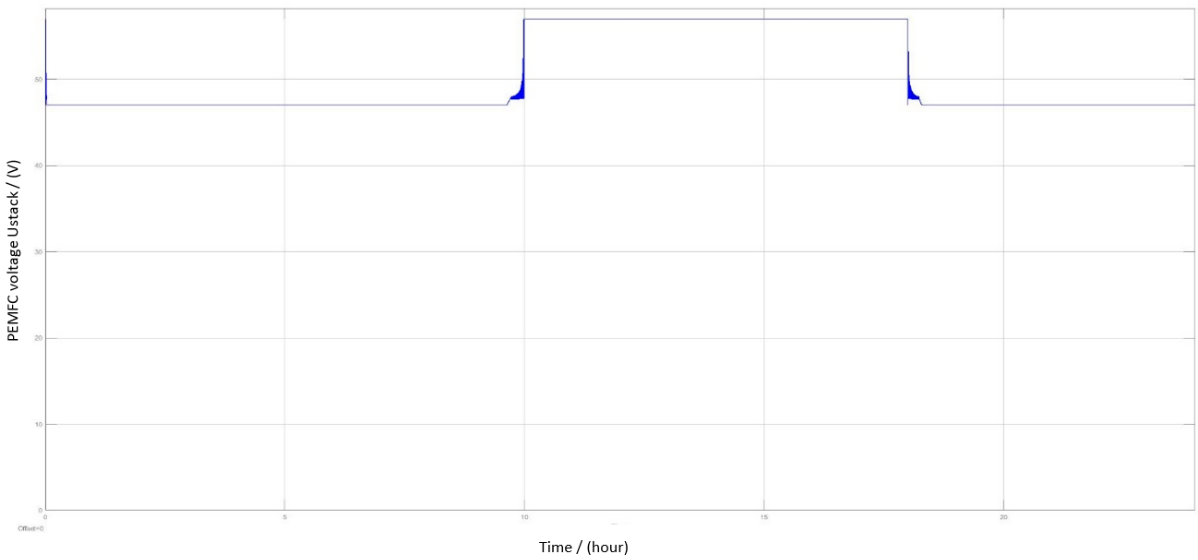

Figure 5.5-3 The output variation of the Voltage in PEMFC with the time

Figure 5.5-4 shows the dynamic change of FC voltage when the FC goes from off state to on state and fuel cell takes nearly 1 s to reach nominal value.

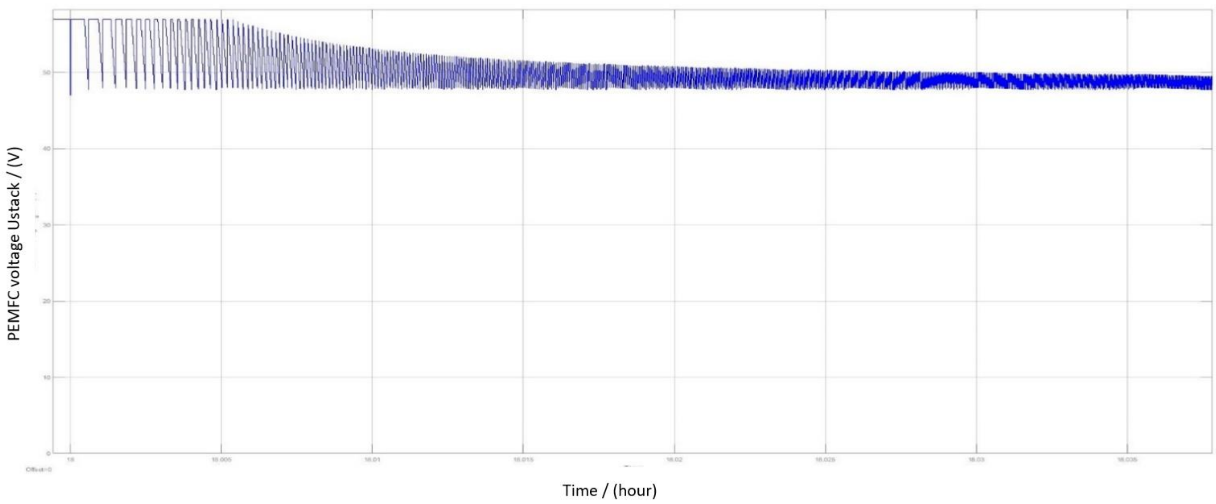

Figure 5.5-4 The output variation of Voltage in PEMFC when the fuel cell goes off state to on state

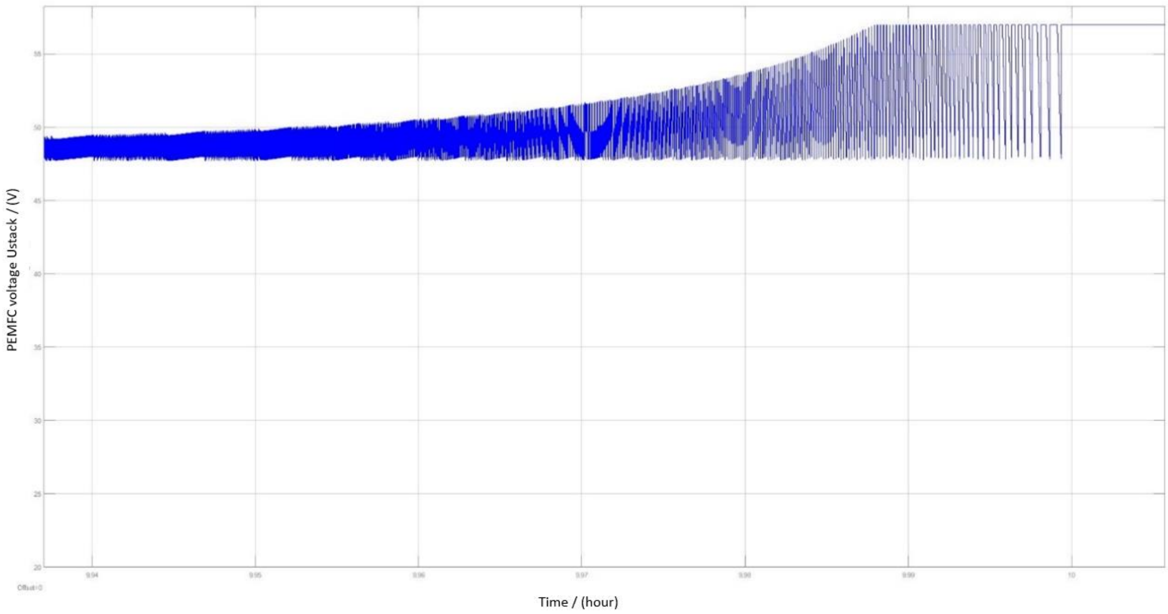

Figure 5.5-5 The output variation of Voltage in PEMFC when the fuel cell goes on state to off state

Figure 5.5-5 shows the dynamic change of FC voltage when the FC goes from on state to off state and fuel cell takes nearly 2 s to reach no load voltage.

Following figure 5.5-6 shows the variation of load voltage with the time. Fuel cell is at off state between 10:00 -18:00.

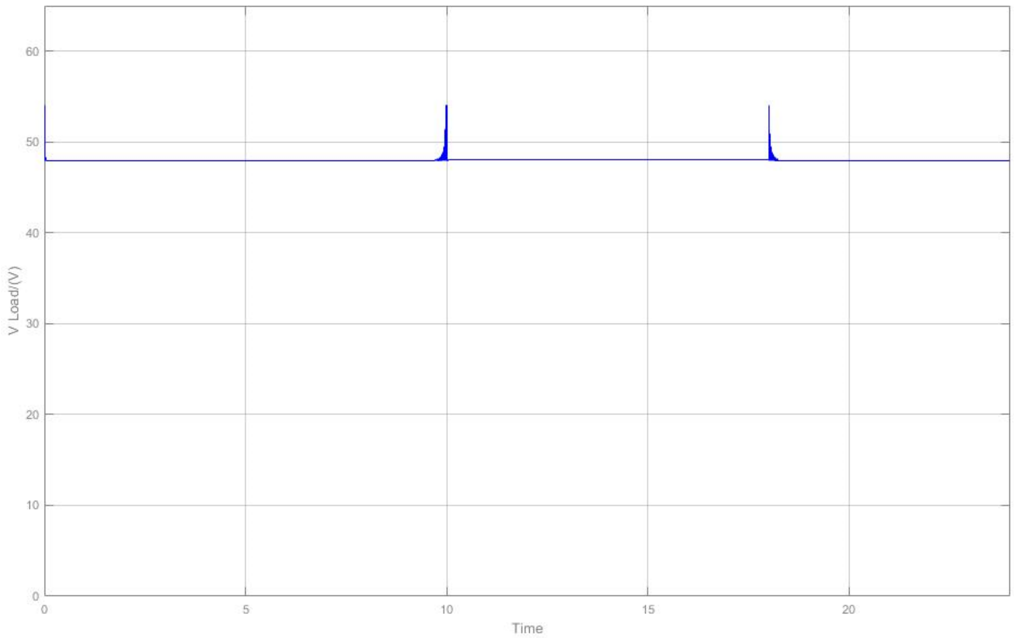

Figure 5.5-6   The output variation of the Load Voltage with the time

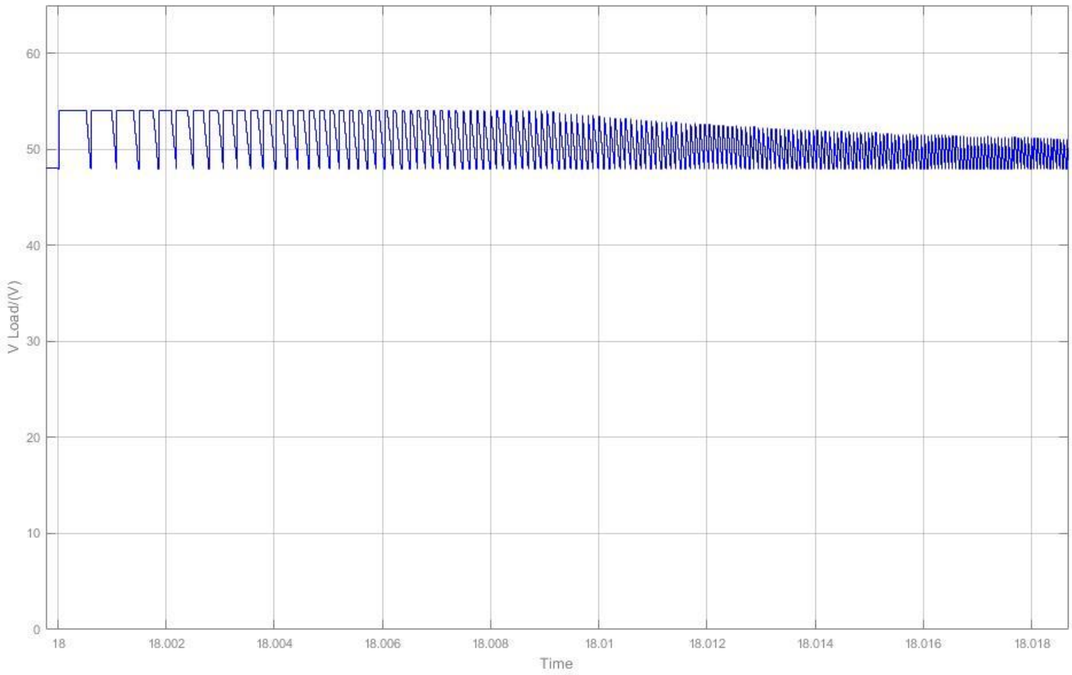

Figure 5.5-7   Dynamic change of the Load Voltage when the fuel cell goes off state to on state

Figure 5.5-7 shows the dynamic change of load voltage when the fuel cell goes from off state to on state and fuel cell takes 0.93 s to reach nominal value.

Figure 5.5-8 shows the output variation of the open of the valve in the H_2 tank.

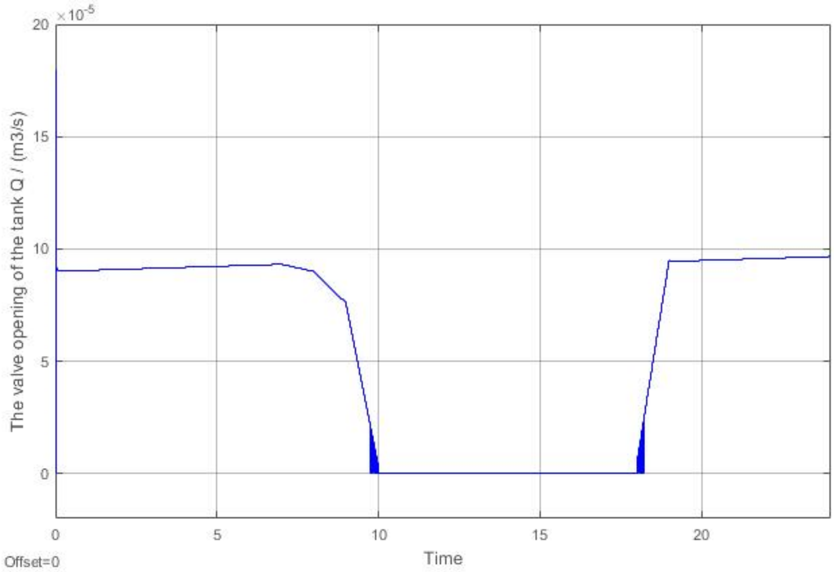

Figure 5.5-8 The output variation of the open of the valve in H_2 Tank

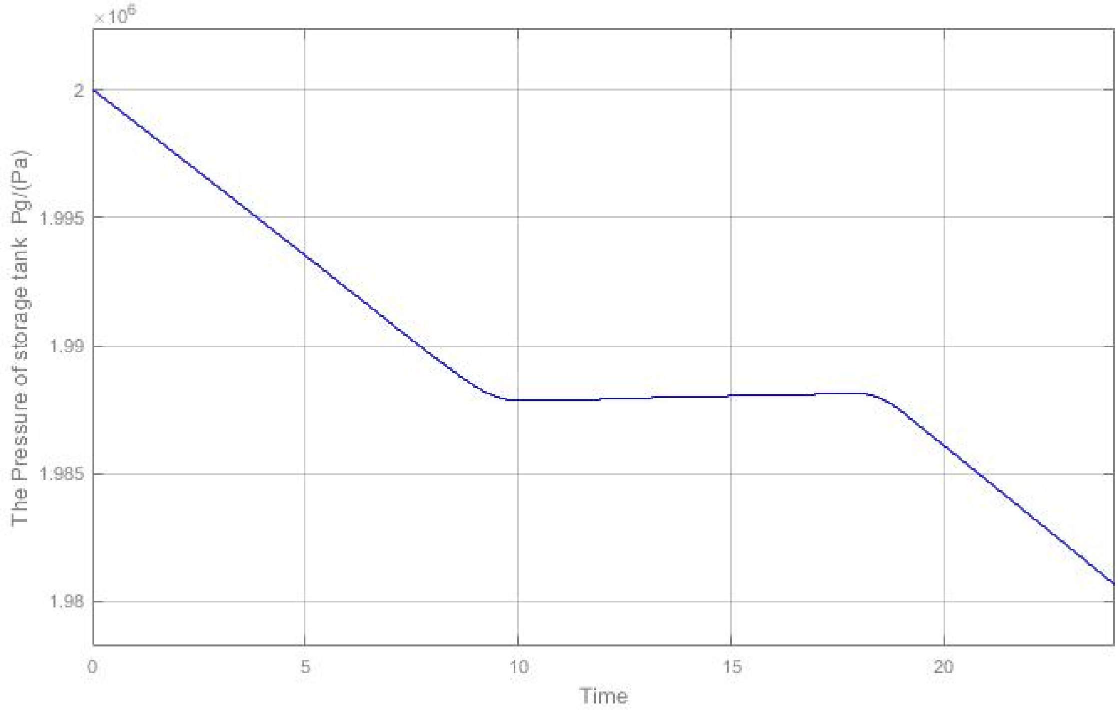

Figure 5.5-9 The output variation of the Pressure in the H_2 Tank with the time

Figure 5.5-9 shows the output variation of the H_2 pressure in H_2 tank.

5.6 Results of the Battery Model

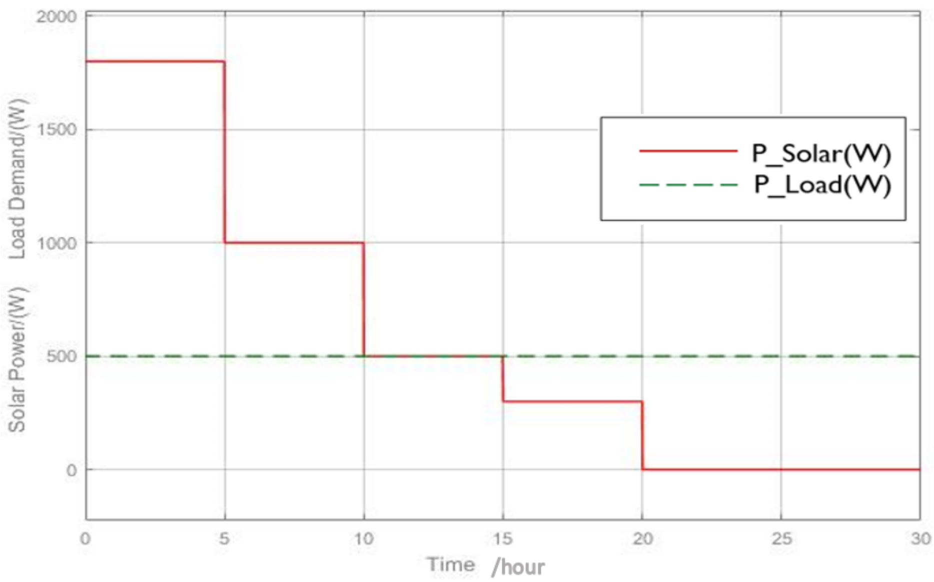

Figure 5.6-1 Solar Power and Load Demand

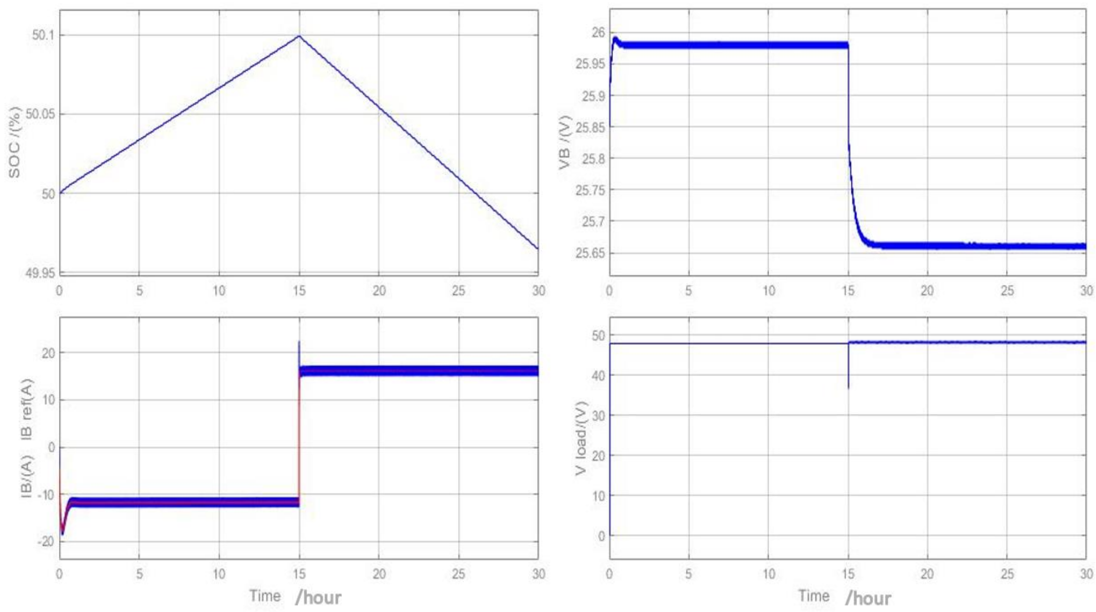

Figure 5.6-2 The Variation of SOC, battery current, battery voltage and load voltage with the time

Figure 5.6-2 shows the variation of SOC, battery current, battery voltage and load voltage with the time.

5.7 Analysis for power variation in a day with the battery

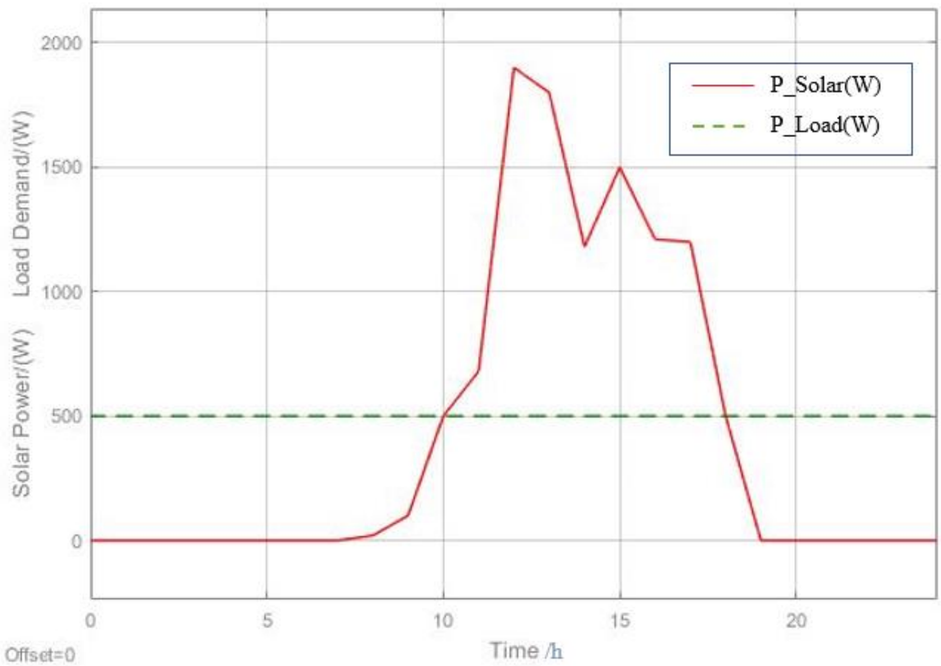

Figure 5.7-1 Solar Power and Load Demand

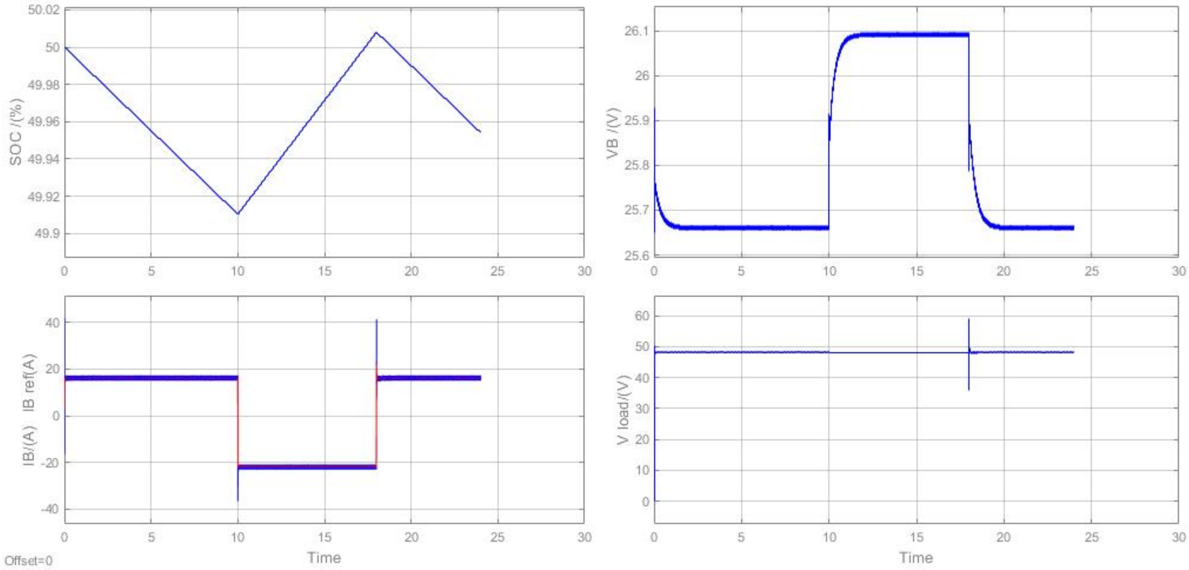

Figure 5.7-2 The Variation of SOC, battery current, battery voltage and load voltage with the time

Figure 5.7-3 shows the dynamic change of SOC, battery current, battery voltage and load voltage when the battery goes from charging state to discharging state. It takes 0.9 s to reach nominal value.

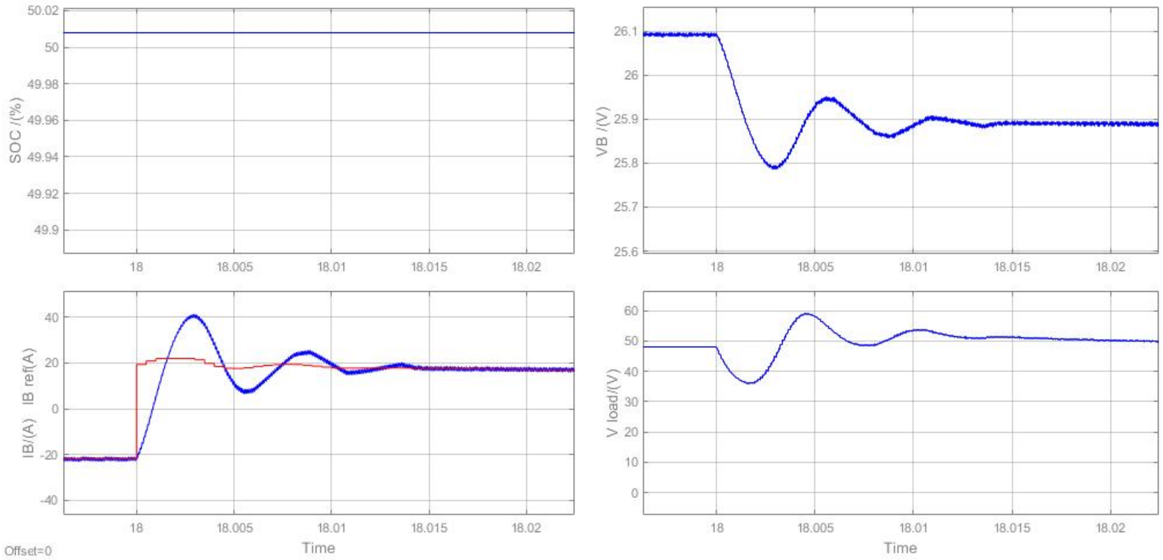

Figure 5.7-3 The Variation of SOC, battery current, battery voltage and load voltage with the time

6. SELECTION OF EQUIPMENTS

6.1 Electrolyzer selection

For the electrolyzer, nel supplier was selected according to our requirements [10].

Figure 6.1-1 The Electrolyzer

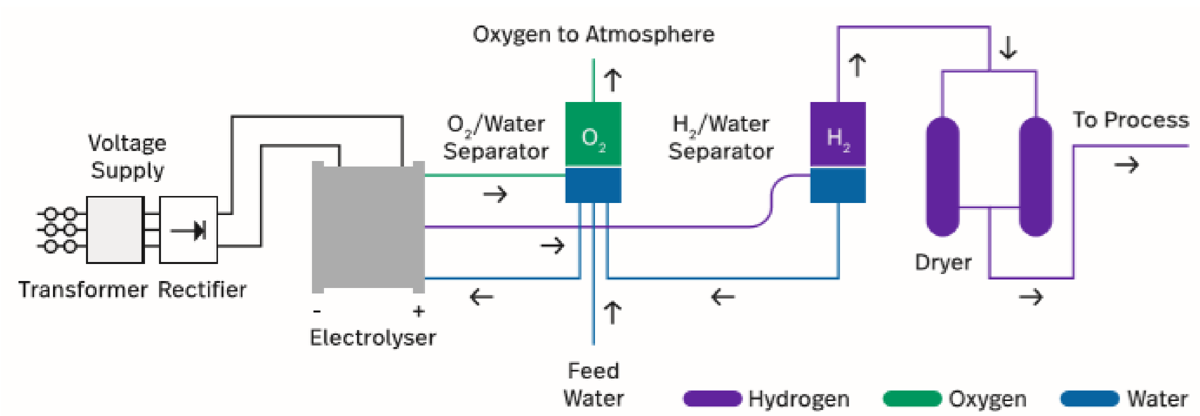

Figure 6.1-1 The process of electrolyzer unit [10]

Table 6.1-1 The specifications of the electrolyzer – S series [10]

SPECIFICATIONS	S10	S20	S40
Nominal Production Rate	0.27 Nm^3/h	0.53 Nm^3/h	1.05 Nm^3/h
Production Capacity Dynamic Range	0-100%	0-100%	0-100%
Power Consumption by System	6.1 kWh/Nm^3	6.1 kWh/Nm^3	6.1 kWh/Nm^3
Purity	99.9995%	99.9995%	99.9995%
O_2-Content in H_2	< 1 ppm v	< 1 ppm v	< 1 ppm v
H_2O-Content in H_2	< 5 ppm v	< 5 ppm v	< 5 ppm v
Delivery Pressure	13.8 barg	13.8 barg	13.8 barg
Dimensions - L x W x H	0.8 m x 1 m x 1.1 m	0.8 m x 1 m x 1.1 m	0.8 m x 1 m x 1.1 m
Ambient Temperature	5-40° C/5-50° C option	5-40° C	5-40° C
Electrolyte	Proton Exchange Membrane	Proton Exchange Membrane	Proton Exchange Membrane
Feed Water Consumption	0.9 l/Nm^3	0.9 l/Nm^3	0.9 l/Nm^3

As above table, selected electrolyzer has nominal production rate of 0.2 Nm^3 / h, working temperature of 5 - 40 °C. It's electrolyte is a proton exchange membrane. Also, it has dimensions of 0.8 m x 1 m x 1.1 m, and it is compatible with our system and requirements.

6.2 Fuel cell selection

There are various categories of FCs and figure 6.2-1 shows the volumetric power density of different types of Fuel cells and it clearly see that the PEM (proton exchange membrane**)** has high volumetric power density compared to other types.

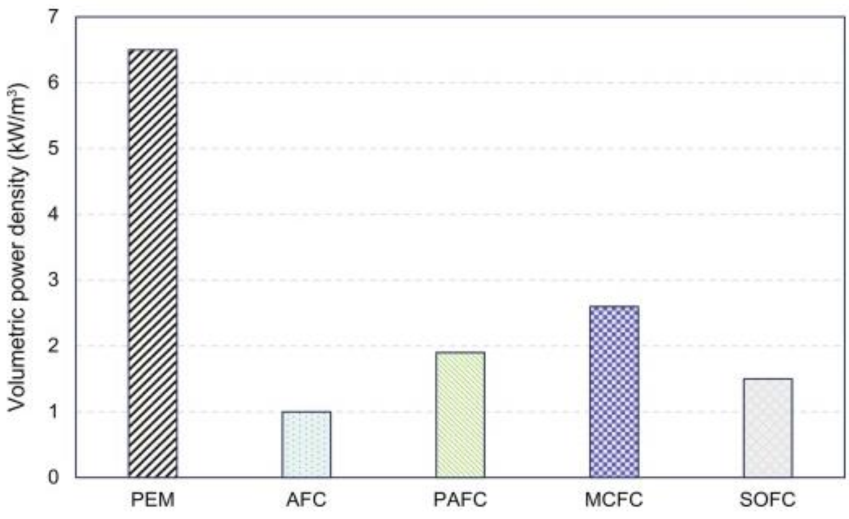

Figure 6.2-1 The volumetric power density of different types of FCs

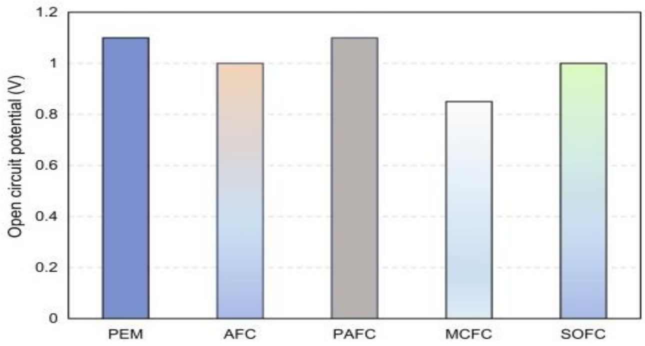

Figure 6.2-2 The open circuit voltage of different types of FCs

Figure 6.2-2 presents the open circuit voltage of various types of FCs.

Not only considering the high volumetric power density, but also due to the following reasons, PEMFC is the best solution.

- starts at room temp.
- Prompt response
- current density is high
- excellent stability
- a long lifespan

PEM fuel cell has the following reactions:

Anode : H_2 (g) → 2H+ (aq) + 2e−

Cathode : ½O_2 (g) + 2H+ (aq) + 2e− → H_2O (l)

Overall : H_2 (g) + ½ O_2 (g) → H_2O (l) + electric energy + waste heat

For the FC, EFOY supplier was selected according to our requirements [14].

Figure 6.2-3 The FC [14]

Table 6.2-1 The specifications of the FC [14]

	JUPITER 2.5
Power output	2500 W
Nominal voltage	48 V DC
Supply voltage	40.5 – 57.0 V DC
Weight	27.0 kg
Connectable H_2 bottles	The system has one connection. Multiple gas-bottles could be connected
Fuel	Hydrogen
Purity of fuel	3.0 or better
Nominal fuel consumption	11 Nl H_2/min/kW
Temperature of air2	-33 °C to +50 °C
Operating height	Up to 3000 m above sea level
Measurements l x w x h	536 x 483 x 311 mm
IP-class	IP 20
Control	Remote Monitoring Tool (optional)
Data-Interface	CAN-Bus

As above table, selected fuel cell has nominal voltage of 48 V, and 2500 W power output. Nominal fuel consumption of the fuel cell is 11Nl H_2/min/kW and it has dimensions of 53.6 cm x 48.3 cm x 31.1 cm, and it is compatible with our system and requirements. Additionally, it has remote monitoring control unit and it's Data-Interface is CAN-Bus. Following is the confirmation of selected fuel cell according to the simulation results:

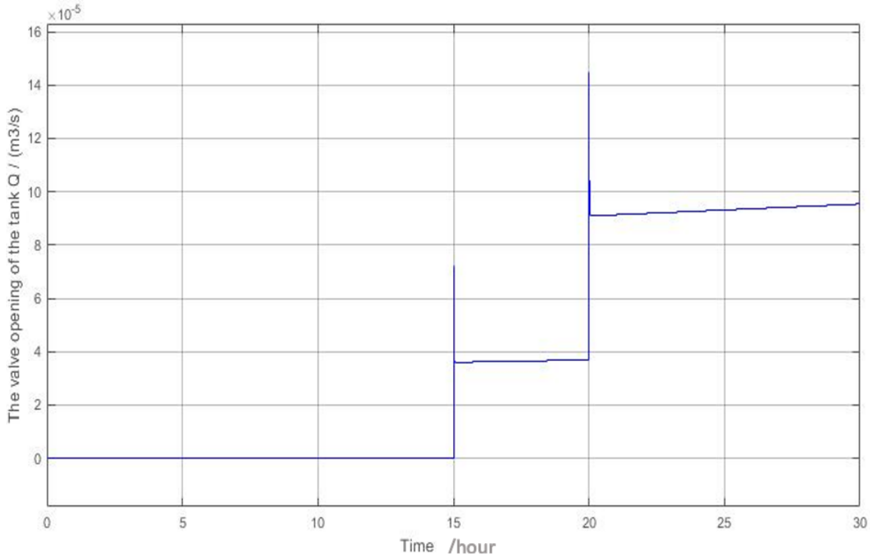

Figure 6.2-4 The output variation of the open of the valve in H_2 Tank with the time

According to the graph :

H_2 consumption rate (Q x t) = $3.6 \times 10^{-5} \times 5 \times 3600 + 9.1 \times 10^{-5} \times 10 \times 3600\ m^3$

= 3924 liters

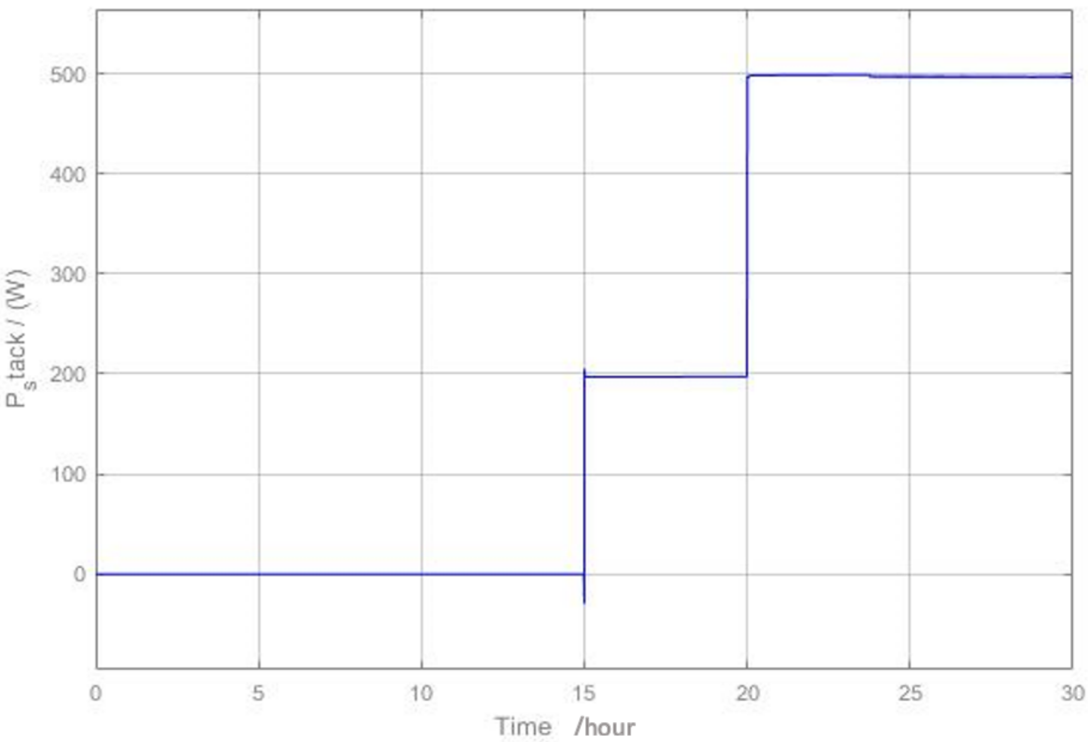

Figure 6.2-5 The output variation of the power of the FC with the time

According to the graph :

P_{stack} x time = 0.199 x 5 + 0.5 x 10 (kW x h)

= 5.995 kW.h

= 359.7 kW.min

From the Technical Data EFOY Hydrogen 2.5 Nominal fuel consumption is 11 Nl H_2/min/kW.

According to that, H2 consumption rate = 359.7 x 11

= 3956.7 liters

When comparing the calculated values from simulation results and the calculated values from the technical data, those values are nearly equal.

6.3 Hydrogen tank selection

Under ambient conditions, 1 m^3 of hydrogen provides 3 kWh it is equivalent to 0.003 kWh/litre [13].

Pressurized hydrogen contains [13]:

- 0.5 kWh/litre at 200 bar
- 1.1 kWh/litre at 500 bar
- 1.4 kWh/litre at 700 bar

Required Volumes to Store 1 kg of H_2 as Compressed Gas at 20 °C are as follow [13]:

Pressure MPa	Volume Liters
0,1013	11,934.0
100	128.7
200	68.4
300	48.4
350	42.7
450	34.9
700	25.7

For the hydrogen tank, MAHYTEC supplier was selected according to our requirements.

MAHYTEC
Innovative Energy Solutions

Figure 6.3-1 The Hydrogen tank [7]

Table 6.3-1 The specifications of the Hydrogen tank [7]

TERMS OF SERVICE					
Maximum working pressure (PS)	500bar				
Maximum refilling pressure	500bar				
Temperature of use	From -40°C to 65°C				
Position of use	Vertical or horizontal				
Permeation rate	0.1Ncm³/h/L				
DIMENSIONS					
Inner volume	140L	160L	200L	250L	300L
Mass of empty tank	130Kg	150Kg	180Kg	210Kg	240Kg
Mass of hydrogen stored at 500b (15°C)	4.5Kg	5Kg	6.5Kg	8Kg	9.5Kg
External dimensions (cm) (without support)	∅ 48 L 158	∅ 48 L 180	∅ 48 L 222	∅ 48 L 263	∅ 48 L 307
Thread Int.	1" - ½ - 12UNF				
MATERIALS					
Body material	Type IV polymer liner with carbon composite				
Boss (x2)	Stainless steel – Aluminum alloy				
REGULATION TEST					
Service life	10 years / 5,000 cycles				
Hydraulic pressure proof test	750bar				
Approved according to	EN12245 – PED 2014/68/EU & TPED 2010/35/EU				
OPTIONS					
Plug	Thread on request				
Valve	PED or TPED				
PRV	Maximum 500 bar				
Fitting rack	Simple (configuration in bundle possible)				

As above table, selected hydrogen tanks have maximum working pressure of 500 bar, working temperature of -40 – 65 °C, inner volumes of 140, 160, 200, 250 and 300 litres and the masses of hydrogen stored at 500 bar of 4.5, 5, 6.5, 8, 9.5 kg. All the tanks have diameter of 48 cm and length of 158, 180, 222, 263, 307 cm.

7. ECONOMICAL ANALYSE

Economic analysis was done by using HOMER tool.

7.1 HOMER tool

By using HOMER tool optimum design can be determined and It gives the creator the freedom to choose the components of the system he wants. Also It compares the other data and calculates the best sizes for the components that the designer desired.Also HOMER tool shows how much energy each component consumed or produced, as well as how long each equipment was in operation. Below figure 7.1-1 depicts how the HOMER tool is being used to simulate the system components [3].

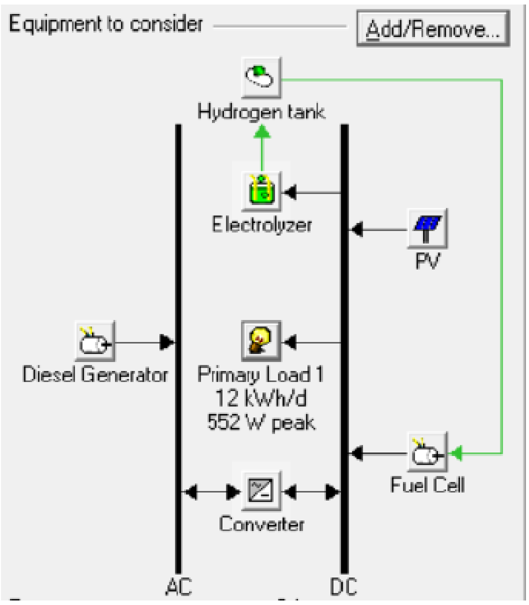

Figure 7.1-1 System modeled in HOMER [3]

When the GPS coordinates of a location are input, it pulls the solar radiation pattern from the web for that area. It estimates the solar intensity's scaled yearly average for the specified location.

7.2 Results

<u>1st Test case</u>

- Site location : Amunakole
- Load demand : 0.5 kW

Optimal solution is as below with increased solar PV and H_2 storage system [3].

System architecture

PV Array	30 kW
Diesel Generator	1 kW
Fuel Cell	1 kW
Inverter	1 kW
Rectifier	1 kW
Electrolyzer	20 kW
Hydrogen Tank	80 kg

Cost summary

Total net present cost	$ 72,741
Levelized cost of energy	$ 1.299/kWh
Operating cost	$ 2,399/yr

Diesel Generator

Quantity	Value	Units
Hours of operation	0	hr/yr
Number of starts	0	starts/yr
Operational life	1,000	yr
Capacity factor	0.00	%
Fixed generation cost	0.610	$/hr
Marginal generation cost	0.250	$/kWhyr

Electrical

Component	Production (kWh/yr)	Fraction
PV array	47,390	96%
Diesel Generator	0	0%
Fuel Cell	2,226	4%
Total	49,616	100%

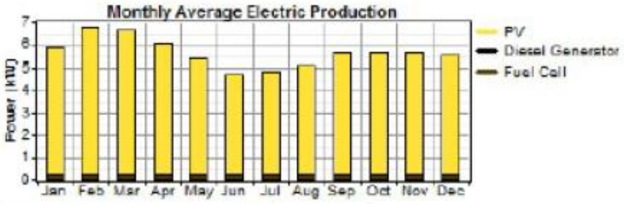

Load	Consumption (kWh/yr)	Fraction
DC primary load	4,380	9%
Electrolyzer load	43,492	91%
Total	47,872	100%

Quantity	Value	Units
Excess electricity	1,744	kWh/yr
Unmet load	0.000000209	kWh/yr
Capacity shortage	0.00	kWh/yr
Renewable fraction	1.000	

Fuel Cell

Quantity	Value	Units
Hours of operation	4,547	hr/yr
Number of starts	375	starts/yr
Operational life	3.30	yr
Capacity factor	25.4	%
Fixed generation cost	0.433	$/hr
Marginal generation cost	0.00	$/kWhyr

Configuration 2 without H_2 storage system is as below [3]:

System architecture

PV Array	2 kW
Diesel Generator	1 kW
Inverter	1 kW
Rectifier	1 kW

Cost summary

Total net present cost	$ 84,590
Levelized cost of energy	$ 1.511/kWh
Operating cost	$ 6,375/yr

Diesel Generator

Quantity	Value	Units
Hours of operation	8,760	hr/yr
Number of starts	1	starts/yr
Operational life	1.71	yr
Capacity factor	46.1	%
Fixed generation cost	0.610	$/hr
Marginal generation cost	0.250	$/kWhyr

In table 7.2-1 it shows that HOMER tool gives the optimum solution as configuration 1 with increased solar PV and H_2 storage system and configuration 2 shows the system components and it's cost without solar system (Present situation). When comparing total annual cost, we can see that the configuration 1 with increased solar PV and H_2 storage system is economically feasible than configuration 2. Also, in 1st case we can totally omit the diesel generator for the test case 1 by seeing the results.

Table 7.2-1 Comparison of the cost of both configurations with HOMER tool [3]

Option 01 - Configuration						
	Capex ($)	Operated Time (Hours)	Opex ($)	Installed capacity (kW)	Electricity Generated	Annual Fuel Consumption (kg/yr)
Solar PV	20,000	4368	30	30	48,841	
Fuel Cell	5,500	4547	455	1	2,300	920
Hydrogen Storage	480		80	80		
Converter	600		40	1	-	
Electrolyzer	15,000		40	20	41,400	
Diesel generator	500	0	100	1	-	
Site Power Load (kW)	0.5					
Telecom energy Consumption (kWh/Yr)	4,380					
		Output of HOMER				
Total generation (kWh/Yr)		49,616				
Total consumption (kWh/Yr)		47,872				
Excess electricity Generated (kWh/Yr)		1,744				
Total Capex - net Present ($)		42,080				
Total Capex - Annualized ($)		3,292				
Total O&M		566				
Fuel cost						
Total OPEX		566				
Total Annual Cost ($) (Option 1)		3,858				

Option 2 - Configuration						
	Capex ($)	Operated Time (Hours)	Opex ($)	Installed capacity (kW)	Electricity Generated	Annual Fuel Consumption (kg/yr)
Solar PV	2,000	4368	102	2	3,256	
Fuel Cell	-	0	-	0	-	0
Hydrogen Storage	-		-	0		
Converter	600		40	1	-	
Electrolyzer	-		-	0	-	
Diesel generator	500	8760	4,480	1	4,030	
Site Power Load (kW)	0.5					
Telecom energy Consumption (kWh/Yr)	4,380					
		Output of HOMER				
Total generation (kWh/Yr)		7,196				
Total consumption (kWh/Yr)		4,380				
Excess electricity Generated (kWh/Yr)		2,343				
Total Capex - net Present ($)		3,100				
Total Capex - Annualized ($)		243				
Total O&M		4383				
Fuel cost		1,710				
Total OPEX		6,093				
Total Annual Cost ($) (Option 2)		6,336				

7.3 Levelized cost

Following is the levelized cost calculation for 10 years for both configuration 1 with increased solar PV and H_2 storage system and configuration 2 without H_2 storage system.

Levelized cost for configuration 1 with increased solar PV and H_2 storage system:

Levelized cost = (Total annual cost x 10 + Fuel cell replacement cost
+ Electrolyzer replacement cost + compressor cost + safety cost)/
(10 x annual energy consumption)
= (3858 x 10 + 5500 + 15000 + 650 + 700) / (10 x 4380)
= 60430 / 43800
= 1.379 $/kWh

Levelized cost for configuration 2 without H_2 storage system:

Levelized cost = (Total annual cost x 10 + Battery replacement cost x 3)/
(10 x annual energy consumption)
= (6336 x 10 + 300 x 3) / (10 x 4380)
= 64260 / 43800
= 1.467 $/kWh

When comparing the levelized cost, we can see that the configuration 1 with increased solar PV and H_2 storage system is economically feasible than configuration 2.

8. RE-SIZING THE EQUIPMENTS AFTER THE COST OPMIZATION

8.1. Matlab simulation results after the increasing size of Solar PV and Electrolyzer

After cost optimization we can clearly see that the size of solar PV and size of the electrolyzer has been increased. Due to that again model in MATLAB simulation was run with new system components and results are as below:

1st test case

Load demand - 0.5 kW

Modified system components are as below:

PV array	30 kW
Fuel cell	2.5 kW
Electrolyzer	20 kW
Hydrogen tank	4.5 kg

The variation of solar PV production is shown in Figure 8.1-1, and the load variation is assumed to be constant throughout the day.

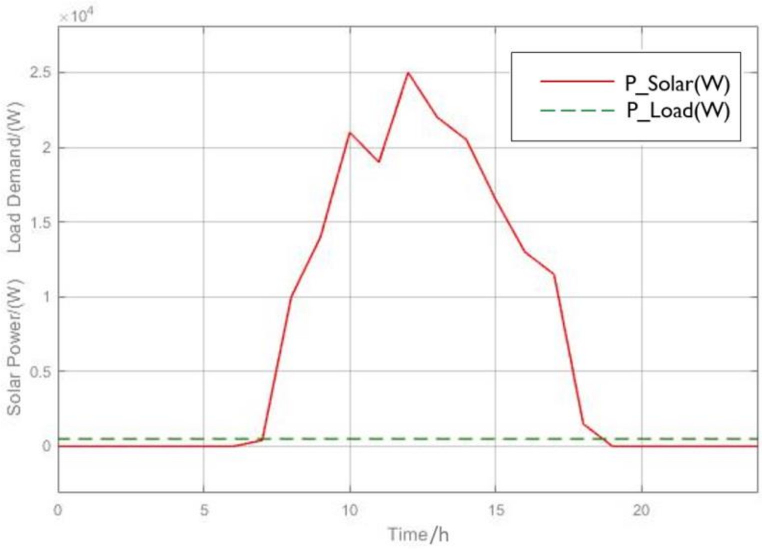

Figure 8.1-1 Solar Power and Load Demand – After modifying the system components

Figure 8.1-2 shows the output variation of the H_2 produced in electrolyzer.

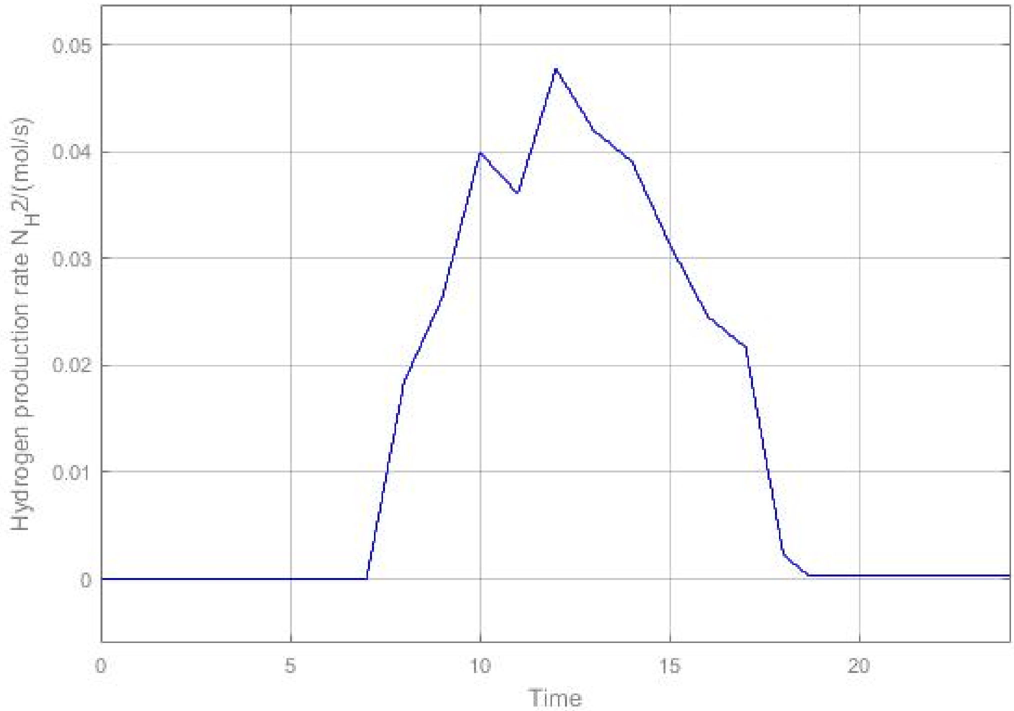

Figure 8.1-2 The output variation of H_2 Production in Electrolyzer with the time– After modifying the system components

Figure 8.1-3 shows the output variation of the voltage in PEMFC with the time.

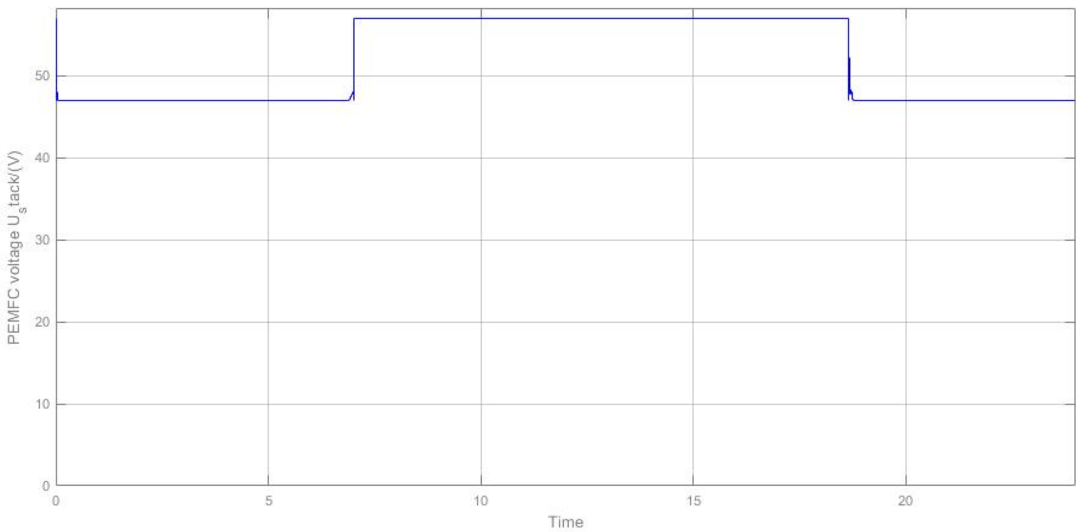

Figure 8.1-3 The output variation of the Voltage in PEMFC with the time– After modifying the system components

Figure 8.1-4 shows the output variation of the current in PEMFC with the time.

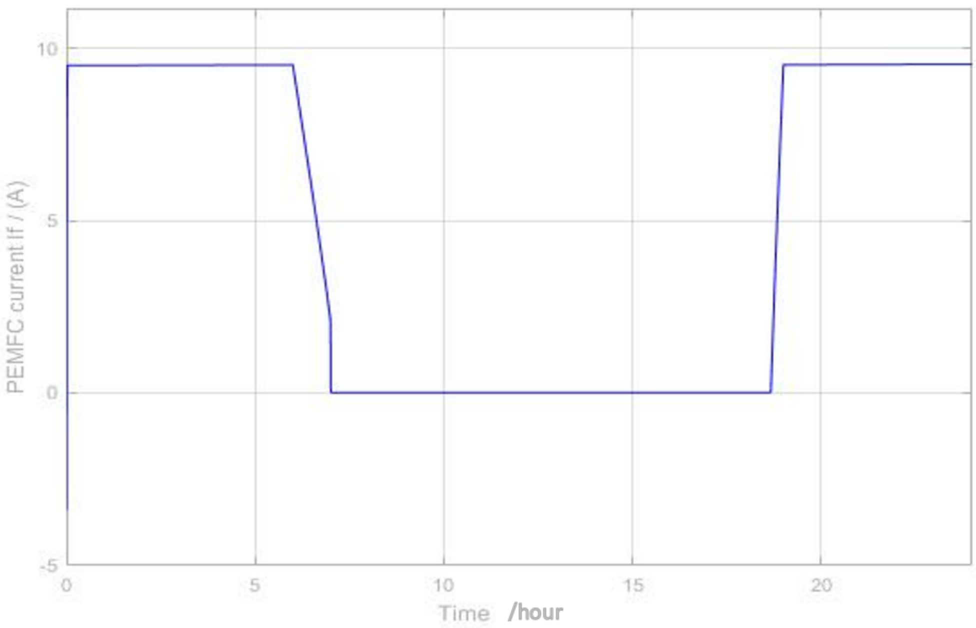

Figure 8.1-4 The output variation of the Current in PEMFC with the time– After modifying the system components

Figure 8.1-5 shows the output variation of the open of the valve in the H_2 tank.

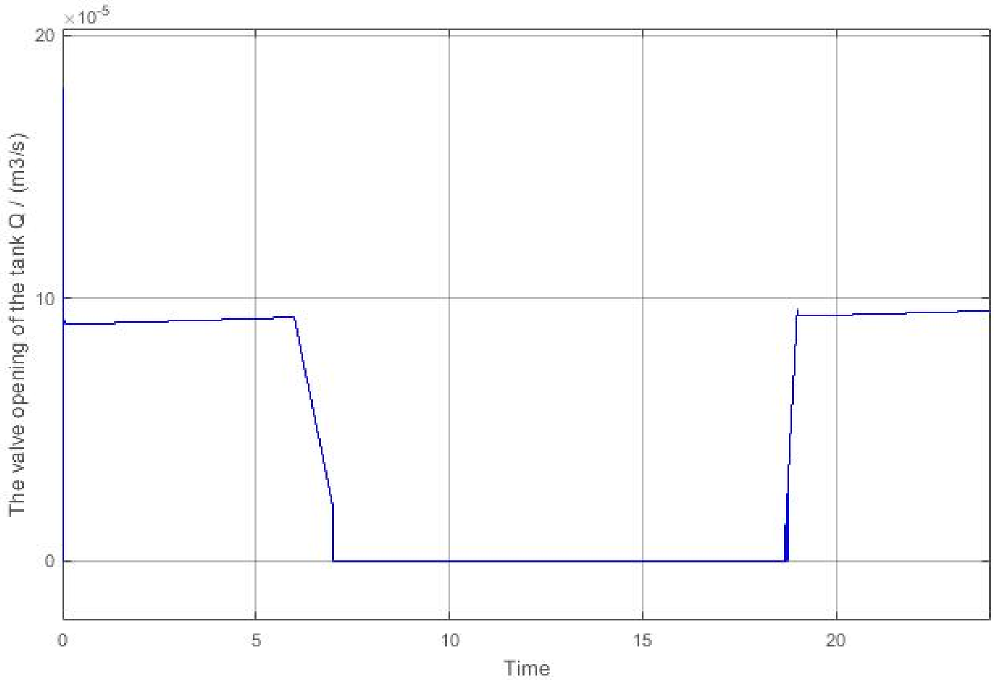

Figure 8.1-5 The output variation of the open of the valve in H_2 Tank with the time– After modifying the system components

Figure 8.1-6 shows the output variation of the H_2 pressure in H_2 tank.

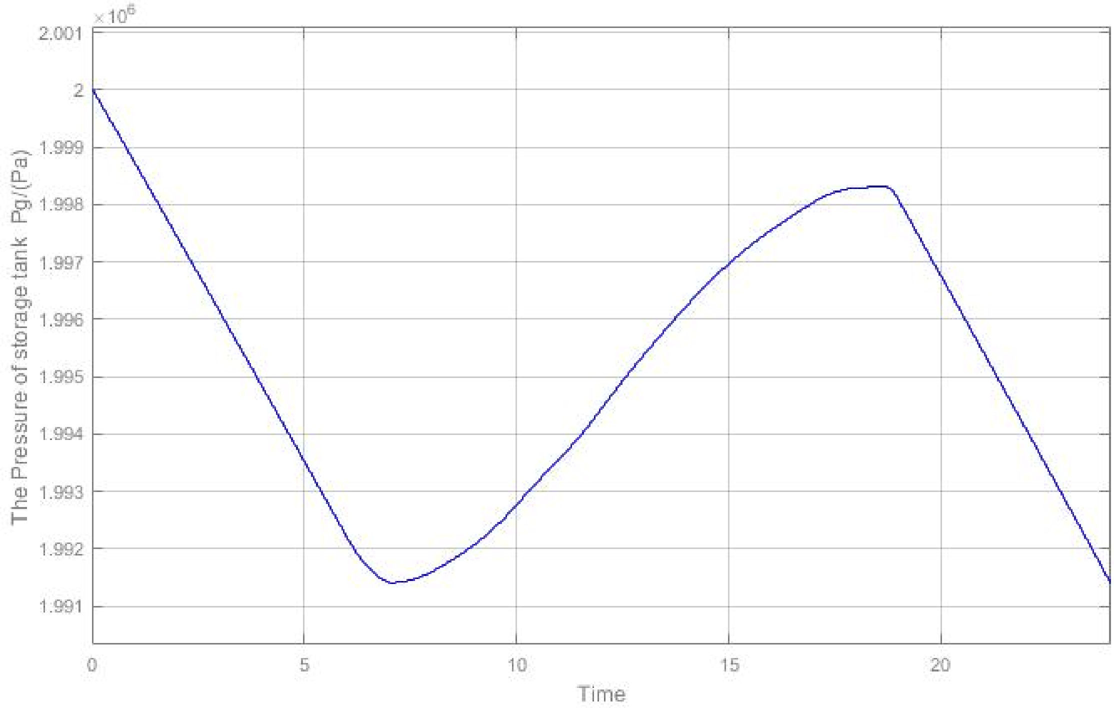

Figure 8.1-6 The output variation of the Pressure in H_2 Tank with the time– After modifying the system components

With the increasing the size of the electrolyzer, we can go for H series electrolyzer in nel supplier.

Table 8.1-1 The specifications of the electrolyzer – H series [10]

SPECIFICATIONS	H2	H4	H6
Nominal Production Rate	2 Nm³/h	4 Nm³/h	6 Nm³/h
Production Capacity Dynamic Range	0-100%	0-100%	0-100%
Power Consumption by System	7.3 kWh/Nm³	7 kWh/Nm³	6.8 kWh/Nm³
Purity	99.9995%	99.9995%	99.9995%
O_2-Content in H_2	< 1 ppm v	< 1 ppm v	< 1 ppm v
H_2O-Content in H_2	< 5 ppm v	< 5 ppm v	< 5 ppm v
Delivery Pressure	15 barg/30 barg option	15 barg/30 barg option	15 barg/30 barg option
Dimensions – L x W x H	1.8 m x 0.8 m x 1.9 m	1.8 m x 0.8 m x 1.9 m	1.8 m x 0.8 m x 1.9 m
Ambient Temperature	5-50⁰ C	5-50⁰ C	5-50⁰ C
Electrolyte	Proton Exchange Membrane	Proton Exchange Membrane	Proton Exchange Membrane
Feed Water Consumption	0.9 l/Nm³	0.9 l/Nm³	0.9 l/Nm³

9. SAFETY-RELATED ISSUES AND BEST PRACTICES

9.1. Hydrogen main hazards

9.1.1 Fire

By its very nature, H_2 is incredibly flammable, requiring very little energy to ignite. In reality, if H_2 gas is leaking at a high pressure from a pipe, it can self-ignite without the need for additional energy. H_2 has a broad range of flammability and can combine explosively with air, as seen in Figure 9.1.1-1. (When in touch with O_2). In reality, mixtures containing as little as 4 % v/v H_2 (the Lower Explosive Limit (LEL)) to 75 % v/v H_2 (the Upper Explosive Limit (UEL)) can cause a flame to spread [11].

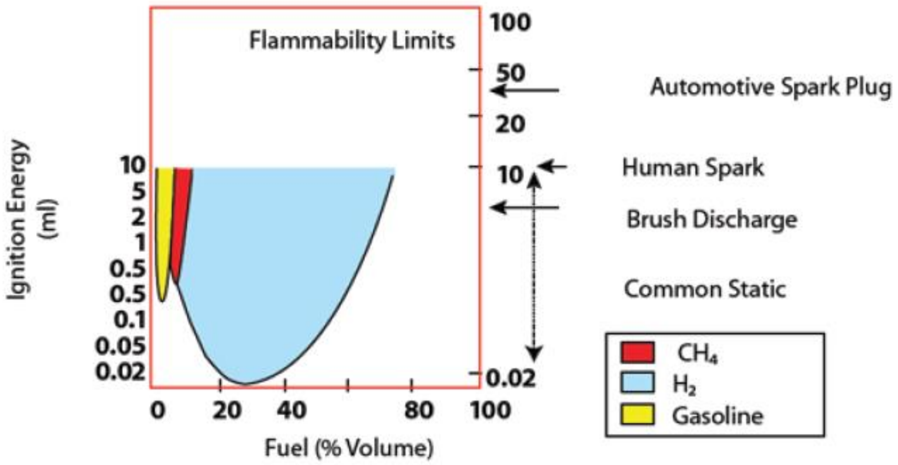

Figure 9.1.1-1 Limits of Flammability and ignition energy of CH_4 (or NG), H_2 and gasoline [11]

9.1.2 Explosion

H_2 can be explosive at quantities ranging from 18.3 % to 59 %. Although the range is wide, it's worth mentioning that gasoline is more dangerous because it can explode at much lower concentrations, ranging from 1.1 % to 3.3 %. Furthermore, because H_2 has a penchant for fast rising, the chances of it exploding in the open are remote. Heavy gases like propane or gasoline vapors, on the other hand, tend to hover near the ground and pose a greater risk of explosion [11].

A fast release of energy followed by pressure waves characterizes an explosion. An explosion, on the other hand, cannot occur in a tank containing solely hydrogen because an oxidizer, such as O_2, must be present in a concentration of at least 10 % pure O_2 or 41 % air for an explosion to occur [11].

9.1.3 Leaks

Leaks must be contained. The main source of worry is hydrogen emissions in areas where it is not planned. When a leak is predicted in a certain area, safety systems are activated. A leak in this area will not be a concern until it has accumulated. Because it displaces oxygen from the air, hydrogen, like any other gas, is asphyxiant if it accumulates in large volumes in a confined space [11].

9.2 General safety practices

9.2.1 Warning signs

This is a popular security technique when working with extreme temperatures and weights, like in the case of hydrogen plants, but not when it comes to hydrogen generation. Caution should be used, and all posted warning signs should be followed. Non-authorized personnel should not enter the ranges marked with these symbols [11].

Figure 9.2.1-1 warning sign [11]

9.2.2 Monitoring systems

Monitoring systems are the most prevalent device used to prevent fires. This apparatus is used as a safety precaution to detect hydrogen or its invisible fire.

Flame detectors that detect UV light from unseen flames are known as ultraviolet (UV) flame detectors [11].

Figure 9.2.2-1 Flame detector [11]

Furthermore, gaseous hydrogen is imperceptible to human senses, and its flames are also imperceptible. As a result, an additional detecting mechanism must be included in the safety device [11].

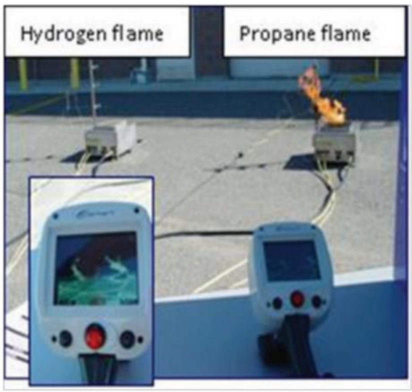

Figure 9.2.2-2 H_2 flame and propane flame [11]

9.2.3 Pressure Relief Devices (PRD)

Pressure relief devices are utilized to release excess pressure that could cause the system to break [11].

CHAPTER 10

10. CONCLUSION

10.1 Conclusion

I have Argued throughout this work that the telecommunication BTS site power system with its all aspects was separately modelled with both Hydrogen storage and battery system. Both storage methods have appeared with nearly similar response time in the dynamic behavior.

In this study, I have explored that the operation of whole system with hydrogen storage system – PEMFC, electrolyzer, Hydrogen tank operation under various test scenarios.

This research study underwent with the real time test results were observed in MATLAB simulation modelling compared with selected equipment specifications, and it was clearly perceived that selected equipment capacities are distinctly viable to install in the area of telecom base stations where the land area is finite.

Furthermore, due to the flammable nature of the H_2 gas, the hydrogen system needs additional safety devices and practices.

Ultimately, entire annual cost of the hydrogen system with extended solar PV is more economically feasible than the system without hydrogen system (the conventional system with battery bank and large amount of diesel generator operating hours).

10.2 Limitations and Assumptions

Limitations:

- Hydrogen system needs additional safety devices whereas battery does not need safety devices
- Equipments Installation also somewhat complex in hydrogen system when comparing to battery system

Assumptions made through the study:

- The load demand of the base station is constant
- The FC is supplied with pure H_2 and air.
- The H_2 and O_2 are ideal and therefore ideal gas law is valid
- The stack's temperature was regulated to be invariant
- The equation of Nernst is valid for the system

REFERENCES

[1] Tesfahunegn S G, Vie P J S, "A Combined Steady State and Dynamic Model of a Proton Exchange Membrane Fuel Cell for use in DG system Simulation, " The 2010 international Power Electronics Conference, pp. 2457- 2464.

[2] Iqbal M T, "Simulation of a small wind fuel cell hybrid energy system, “Renewable Energy, vol. 28, pp. 511-522, 2003.

[3] A. S. Anupama Silva, K.M.T.U. Hemapala, M.A. Kalhan Sandaru Boralessa. "Techno - Economic Analysis of On-Site Hydrogen Production and Storage System with Solar PV for Telecom Sites in Sri Lanka", MSc Thesis, University of Moratura, 2018

[4]Haifeng Liang, Jian Li, Weichao Zhang, Xiaorong Zhu. "Research on full-processmodel of fuel cell generation system", 2012 IEEE International Conference on Power System Technology (POWERCON), 2012

[5] Yan Liujin, "Research on Fuel Cell in Distributed Generation System, “Ph.D. dissertation, Hefei University of Technology, 2009.

[6] Hu Lihua, "Analysis of Fuel Cell Generation System Application, " Ph.D. dissertation, Chongqing University, 2005.

[7] www.mahytec.com (internet source)

[8] Huang, X. Fuel Cell Technology for Distributed Generation: An Overview. In Proceedings of the 2006 IEEE International Symposium on Industrial Electronics, Montreal, QC, Canada, 9–13 July 2006.

[9] Mahapatra, M.K.; Singh, P. Fuel Cells: Energy Conversion Technology. In Future Energy; Elsevier: Amsterdam, The Netherlands; pp. 511–547.

[10] www.nelhydrogen.com (internet source)

[11] www.h2euro.org (internet source)

[12] hal-centralesupelec.archives-ouvertes.fr (internet source)

[13] www.idealhy.eu (internet source)

[14] my-efoy.com (internet source)